



Classical and quantum thermodynamics in a non-equilibrium regime: Application to thermostatic Stirling engine

Shoki Koyanagi ^{a)} and Yoshitaka Tanimura ^{a)}

Department of Chemistry, Graduate School of Science, Kyoto University, Kyoto 606-8502, Japan

(Dated: Last updated: 24 September 2024)

We have developed a thermodynamic theory in the non-equilibrium regime, which we describe as a thermodynamic system-bath model [S. Koyanagi and Y. Tanimura, *J. Chem. Phys.* **160**, 234112 (2024)]. Based on the dimensionless (DL) minimum work principle, non-equilibrium thermodynamic potentials are expressed in terms of non-equilibrium extensive and intensive variables in time derivative form. This is made possible by incorporating the entropy production rate into the definitions of non-equilibrium thermodynamic potentials. These potentials can be evaluated from the DL non-equilibrium-to-equilibrium minimum work principle, which is derived from the principle of DL minimum work and is equivalent to the second law of thermodynamics. We thus obtain the non-equilibrium Massieu–Planck potentials as entropic potentials and the non-equilibrium Helmholtz–Gibbs potentials as free energies. Unlike fluctuation theorem and stochastic thermodynamics theory, this theory does not require the assumption of a factorized initial condition and is valid in the full quantum regime where the system and bath are quantum mechanically entangled. Our results are numerically verified by simulating a thermostatic Stirling engine consisting of two isothermal processes and two thermostatic processes using the quantum hierarchical Fokker–Planck equations and the classical Kramers equation derived from the thermodynamic system-bath model. We then show that, from weak to strong system-bath interactions, the thermodynamic process can be analyzed using a non-equilibrium work diagram analogous to the equilibrium one for given time-dependent intensive variables. The results can be used to develop efficient heat machines in non-equilibrium regimes.

I. INTRODUCTION

Ever since Carnot explored the efficiency of heat engines 200 years ago,¹ there have been longstanding attempts to study thermodynamics in non-equilibrium regimes driven by academic curiosity and practical interest. In particular, recent advances in nanotechnology have led to increased interest in the study of the thermodynamics of microscopic systems.^{2–31}

As a kinetic theory, such phenomena are typically explained using open quantum dynamics theories based on the system–bath (SB) model.^{32–35} Although thermodynamics is a system-independent theory, it is derived from the presence of a heat bath and is consistent with theories based on the SB model.²⁴ The main (subsystem) system of the SB model can be described from a simple two-level system to complex molecular systems with many degrees of freedom, and it is also possible to take the classical limit in the case of a system described in phase space.^{33–40} Under the condition of a heat bath with infinite degrees of freedom, the total system irreversibly relaxes toward its equilibrium state in time, so the second law of thermodynamics is naturally obeyed without the need for the assumption of ergodicity as a dynamical system.^{38–41}

However, to investigate whether the thermodynamic laws are satisfied even in quantum cases where the sub-

system and bath are quantum mechanically entangled, it is necessary to treat the bath in a non-Markovian, non-perturbative, and non-factorized manner so that the thermal equilibrium state of the total system satisfies the energy conservation law, including the SB interaction. Thus, equations of motion derived using the Markovian or rotational wave (or secular) approximation, such as the Lindblad equation and quantum master equation, can only be applied to high-temperature regions where the subsystem exhibits semiclassical dynamics.^{38–41} Therefore, the validity of theories based on the Markov assumption⁴² or those based on factorized initial conditions, such as the fluctuation theorem^{13–15} and stochastic thermodynamics^{16–23} in the quantum case, should be carefully examined.

Over the past 30 years, several methodologies have been developed to accurately describe the effects of quantum entanglement in condensed systems while maintaining strict energy conservation to satisfy the first law of thermodynamics. Such methods include the hierarchical equations of motion (HEOM),^{36–41,43} the quasi-adiabatic path integral (QUAPI),^{44–50} and multiconfigurational time-dependent Hartree (MCTDH),^{51–53} in historical order. Among these, the HEOM approach is ideal for thermodynamic investigations, not only because it can perform numerically “exact” dynamic simulations but also because it can evaluate the change in energy of the heat bath and the SB interaction separately, even for processes far from equilibrium.^{28–31,54–62} Note that although not numerically “exact”, several non-perturbative approaches have also been developed specifically for thermodynamic systems.^{63–65}

^{a)} Authors to whom correspondence should be addressed: koyanagi.syoki.36z@st.kyoto-u.jp and tanimura.yoshitaka.5w@kyoto-u.jp

While the difficulty of numerical simulation has been solved, a fundamental difference exists between open quantum dynamics theory, which is based on a first-principles description of kinetic systems from a microscopic perspective, and thermodynamic theory, which is based on a phenomenological description of thermal systems from a macroscopic perspective. For example, in quantum mechanics, observables are defined as expectation values, whereas in thermodynamics, they are described by macroscopic intensive and extensive variables. Furthermore, quantum mechanics is a formalism for time evolution, whereas thermodynamics deals primarily with static and quasi-static states near thermal equilibrium. In this respect, most quantum thermodynamics studies are merely kinetic simulations of open quantum dynamics, and their relation to thermodynamics has not been studied in depth. Thus, the fundamental difference between microscopic quantum mechanics and macroscopic thermodynamics raises many open questions, such as whether the Carnot limit can be violated in a quantum case or the existence of Maxwell’s demon.

The virtue of thermodynamics lies in its ability to describe macroscopic thermal phenomena resulting from complex microscopic interactions in a system-independent manner, as changes in thermodynamic potentials described as interrelated intensive and extensive variables through Legendre transformations. This virtue should be preserved when developing quantum thermodynamic theory rather than open quantum dynamical theory, although in either case, the theory must be specific to the SB model.

The assumption of a factorized initial state is essential for the application of stochastic thermodynamics and the fluctuation theorem, so that these theories cannot describe the transitions between states in which the system and the bath are entangled. Also, in practice many quantum thermodynamics arguments treat a heat bath perturbatively, assuming Markovian time evolution,^{13–17} it has been found that the Gibbs energy can be obtained directly from kinetic simulations even in the case of non-Markovian and non-perturbative SB interaction at low temperature, where quantum entanglement between the system and the bath plays an essential role.^{28,29,58,59} This approach based on the minimum work principle (or Kelvin–Planck statement), expressed as $W(t) \geq \Delta G(t)$, where $W(t)$ is the work done by the outside on the subsystem by external fields and $\Delta G(t)$ is the change in free energy, by evaluating the work in a quasi-static process,^{28,29} which allows us to draw a work diagram corresponding to the P – V diagram.^{58,59} However, even with this approach, the contributions of temperature T and entropy S to the thermodynamic potential expressed as TdS and SdT cannot be evaluated because the minimum work principle is defined as an isothermal process $dT = 0$.

To overcome this limitation, we developed a thermostatic SB model that is defined by a system coupled to multiple heat baths at different temperatures.^{61,62}

We then extended the minimum work principle to thermostatic processes in a dimensionless (DL) form (the DL minimum work principle) as $\tilde{W}(t) \geq \Delta \Xi(t)$, where $\tilde{W}(t) \equiv \beta(t)W(t)$ is the DL (entropic) work, $\beta(t) \equiv 1/k_{\text{B}}T(t)$ (where k_{B} is the Boltzmann constant) is the time-dependent inverse temperature, and $\Delta \Xi$ is the change in the DL Planck potential.⁶¹ Not only intensive variables but also extensive variables, which are related by time-dependent Legendre transformations, were introduced as quantum expectation values of the SB system.

The validity of these results was verified using the numerically “exact” HEOM formalism. For thermodynamic studies, the HEOM approach has been used for spin-boson-based systems, taking advantage of the ability to evaluate the energy changes of the system, interaction, and bath, respectively, even under non-perturbative and non-Markovian conditions.^{28–31,58–60} Here, we employed the HEOM formalism for an anharmonic quantum Brownian model to construct a thermodynamic theory that is valid for both classical and quantum cases. Restricting to the case of an Ohmic spectral distribution function (SDF), we derived the thermostatic quantum Fokker–Planck equations (T-QFPE)^{61,62} on the basis of the low-temperature quantum Fokker–Planck equations (LT-QFPE) in the quantum case and the Kramers equation in the classical case.⁶⁶ In the classical and high-temperature limits, the T-QFPE are equivalent to the Langevin equation, where a Markovian description can be applicable, but at low temperatures, owing to quantum entanglement with the bath (bathentanglement),⁴⁰ the subsystem follows non-factorial and non-Markovian dynamics, and its equilibrium state deviates from the Boltzmann distribution. This indicates that thermodynamics in the fully quantum regime cannot be described by a theory based on the Markovian assumption.^{60,62}

Although these results were restricted to quasi-static cases, the thermodynamic potentials, intensive and extensive variables, and Legendre transformations were defined in such a way that they hold for any non-equilibrium process. Taking advantage of this, we extend our thermodynamic theory here to the non-equilibrium regime.

The remainder of this paper is organized as follows. In Sec. II, our previous results about thermodynamics as applied to work in a system-independent manner are summarized. We then derive the principle of non-equilibrium DL minimum work to obtain the DL Massieu–Planck potential and Helmholtz–Gibbs potentials in the non-equilibrium regime. Results are verified in Sec. III by numerical simulations using the thermostatic SB model. Finally, Sec. IV presents concluding remarks.

II. REFLECTIONS ON MOTIVE POWER OF HEAT

In our previous paper,⁶¹ we presented system-specific thermodynamic laws described as a system-bath model on the basis of open quantum dynamics theory. Here, we develop the same laws by introducing several ther-

modynamic “statements” without going into the details of the system, as in traditional thermodynamic theory. By doing so, we clarify the distinctive features of thermodynamic theory that allow it to treat systems in non-equilibrium regimes.

A. Laws of thermodynamics applied to work

We consider a thermodynamic system consisting of subsystem A and heat bath B at the inverse temperature $\beta(t)$. The presence of a heat bath temperature can be regarded as a consequence of **the zeroth law of thermodynamics**, which states the existence of a unique equilibrium state.⁶⁷ Although not well known, **the minus first law of thermodynamics** was introduced some time ago to state the existence of time-irreversible processes toward a unique equilibrium state.^{68,69} The dynamics of the SB model comply with this law.

An important statement of thermodynamics is that thermodynamic systems are described in terms of intensive and extensive variables. In particular, extensive variables that are proportional to the size are essential. This statement is called the fourth law.⁶⁷ However, this is the premise of thermodynamics, and we would like to call it **the minus second law of thermodynamics** because this is the central dogma in the classical and quantum thermodynamics that we are constructing.

The energy of the subsystem corresponds to the internal energy and is expressed as $U_A(t)$, which changes with time owing to changes in the bath temperature. Internal energy is an extensive variable, whereas inverse temperature is an intensive variable. The external perturbation considered here is expressed as $-x(t)X_A(t)$, where $x(t)$ and $X_A(t)$ are intensive and extensive variables, respectively. In traditional thermodynamics, $x(t)$ is derived from the Euler relation. We then introduce the total energy, which is related to the enthalpy by $H_A(t) = U_A(t) - x(t)X_A(t)$, which can also be regarded as the Legendre transformation between internal energy and enthalpy.

Because $U_A(t)$ is the conjugate variable of $\beta(t)$, we introduce the DL (or entropic) internal energy denoted by $\tilde{U}_A(t)$, where $\tilde{B}(t) \equiv \beta(t)B(t)$ for any variable $B(t)$. Because $\beta(t)$ diverges for $T \rightarrow 0$, states with $T = 0$ do not exist. Thus the introduction of DL variables corresponds to **the third law of thermodynamics**.

From the time derivative of the DL internal energy $\tilde{U}_A(t)$, we obtain

$$\frac{d\tilde{U}_A(t)}{dt} = \frac{d\tilde{W}_A^{ext}(t)}{dt} + \frac{d\tilde{Q}_A^{ext}(t)}{dt}, \quad (1)$$

where

$$\frac{d\tilde{W}_A^{ext}(t)}{dt} = U_A(t) \frac{d\beta(t)}{dt} + \tilde{x}(t) \frac{dX_A(t)}{dt} \quad (2)$$

and

$$\frac{d\tilde{Q}_A^{ext}(t)}{dt} \equiv \beta(t) \frac{dU_A(t)}{dt} - \tilde{x}(t) \frac{dX_A(t)}{dt}, \quad (3)$$

and $\tilde{W}_A^{ext}(t)$ and $\tilde{Q}_A^{ext}(t)$ represent the DL (or entropic) extensive work defined as being done by the outside and DL (or entropic) extensive heat, respectively. The time derivative of $\tilde{W}_A^{ext}(t)$ corresponds to the DL extensive power. For the enthalpy, we have

$$\frac{d\tilde{H}_A(t)}{dt} = \frac{d\tilde{W}_A^{int}(t)}{dt} + \frac{d\tilde{Q}_A^{ext}(t)}{dt}, \quad (4)$$

where

$$\frac{d\tilde{W}_A^{int}(t)}{dt} \equiv U_A(t) \frac{d\beta(t)}{dt} - X_A(t) \frac{d\tilde{x}(t)}{dt} \quad (5)$$

and $\tilde{W}_A^{int}(t)$ represents the DL intensive work. The time derivative of $\tilde{W}_A^{int}(t)$ then corresponds to the DL intensive power. Equations (1) and (4) correspond to **the first law of thermodynamics**.

From the definitions, these intensive and extensive variables satisfy the time-dependent Legendre (TDL) transformation expressed as follows:

$$\frac{d\tilde{W}_A^{int}(t)}{dt} = \frac{d\tilde{W}_A^{ext}(t)}{dt} - \frac{d}{dt} [\tilde{x}(t)X_A(t)]. \quad (6)$$

Equation (1) can also be expressed in the form of a TDL transformation as

$$\frac{d\tilde{W}_A^{ext}(t)}{dt} = -\frac{d\tilde{Q}_A^{ext}(t)}{dt} + \frac{d}{dt} [\beta(t)U_A(t)]. \quad (7)$$

The DL intensive heat $\tilde{Q}_A^{int}(t)$ can also be defined from $\tilde{Q}_A^{ext}(t)$ using the TDL [Eq. (A2) in Appendix A]. The above equations, including the first law of thermodynamics, are described in terms of intensive variables $\beta(t)$ and $\tilde{x}(t)$ and extensive variables $U_A(t)$ and $X_A(t)$ and hold for any non-equilibrium processes. While these intensive and extensive variables are the state variables because they are kinetic observables at time t , work and heat are not state variables.

As **the second law of thermodynamics**, we adopt **the DL minimum work principle** for the subsystem moving from one equilibrium state to another, thereby extending the Kelvin–Planck statement for isothermal processes to thermostatic processes. For work defined as being performed from the outside on the subsystem, we have

$$\tilde{W}_A^{ext} \geq -\Delta\Phi_A^{qst}, \quad (8)$$

where Φ_A^{qst} is the DL Massieu potential^{70,71} and equality holds under quasi-static changes in the natural variables $\beta(t)$ and $X_A(t)$ as $\Phi_A^{qst}[\beta^{qst}, X_A^{qst}] = \tilde{W}_A^{ext}[\beta^{qst}, X_A^{qst}]$. The above inequality states that for any process occurring between two states, the work done by the outside

is minimized if the process is quasi-static (or reversible) because no energy is dissipated in the heat bath. Note that if we define work as being done by the subsystem on the outside, the inequality in Eq.(8) is reversed, and the relationship is called the maximum work principle (on the outside). Although not mathematically rigorous, the derivation of Eq. (8) is described in Appendix A of Ref. 61. Using the TDL transformation (6), we also obtain the Planck potential^{71,72} in terms of natural variables expressed as $\Xi_A^{\text{qst}}[\beta^{\text{qst}}, \tilde{x}^{\text{qst}}]$ (see Appendix A). Similar expressions for Planck functions were derived on the basis of stochastic thermodynamics.^{19,21,22} However, our expression was obtained from the well-defined kinetic system and is valid even under non-factorized SB interactions, where bathentanglement plays an essential role. Thus, the value of $\Delta\Phi_A^{\text{qst}}$ appearing in Eq. (8) is generally different from the value evaluated from stochastic thermodynamics.

For the DL extensive heat $\tilde{Q}_A^{\text{ext}}(t)$, we have

$$\tilde{Q}_A^{\text{ext}} \leq \Delta\Lambda_A^{\text{qst}}, \quad (9)$$

which corresponds to **the principle of maximum entropy**, where $\Lambda_A^{\text{qst}}[U_A^{\text{qst}}, X_A^{\text{qst}}]$ is the entropic potential. Because both natural variables are extensive, this potential is fundamental and we call it the Massieu entropy (M-entropy). Using the TDL transformation given by Eq. (A2), we also obtain the Planck entropy (P-entropy) defined by $\Gamma_A^{\text{qst}}[U_A^{\text{qst}}, \tilde{x}^{\text{qst}}]$ from $\tilde{Q}_A^{\text{int}}(t)$ (see Appendix A). Similar to the entropy obtained from the partition function in statistical physics, this entropy is a function of the intensive variable \tilde{x}^{qst} .

Here, as the conjugate variable for $\beta(t)$, we chose the internal energy U_A^{qst} , which is considered a fundamental variable in thermodynamics. As demonstrated in our previous paper,⁶¹ enthalpy H_A^{qst} could also be chosen as the conjugate variable for $\beta(t)$. In such a case, there are also two entropies, one involving both extensive variables (Clausius entropy or C-entropy) and one intensive variable with respect to external forces (Boltzmann entropy or B-entropy). The B-entropy and M-entropy values are related to the others by Legendre transformations between U_A^{qst} and H_A^{qst} and the values do not change, although the former includes one intensive variable, whereas the latter includes extensive variables only. However, there is no explicit relationship between C-entropy and M-entropy, because the Legendre transformations between two entropies in the U_A^{qst} representation and the H_A^{qst} representation are different. (See Appendix D in Ref. 61). The Massieu and Planck potentials are equivalent to the entropy potentials introduced earlier.⁷³

The total differential form of the Helmholtz–Gibbs potentials can be derived from the Massieu–Planck potentials using the definitions $F_A^{\text{qst}}(t) = -\Phi_A^{\text{qst}}(t)/\beta^{\text{qst}}(t)$ and $G_A^{\text{qst}}(t) = -\Xi_A^{\text{qst}}(t)/\beta^{\text{qst}}(t)$. The results are summarized in Table VI in Appendix A.

B. Thermodynamic potentials in a non-equilibrium regime

1. The DL non-equilibrium minimum work principle

On the basis of Eq. (8), we define thermodynamic potentials applicable to the non-equilibrium regime. Consider a non-equilibrium state A and equilibrium state n . **The DL non-equilibrium-to-equilibrium minimum work principle** for $A \rightarrow n$ is expressed as (see Appendix B)

$$(\tilde{W}_A^{\text{ext}})_{A \rightarrow n} \geq -(\Delta\Phi_A^{\text{neq}})_{A \rightarrow n}, \quad (10)$$

where $\Phi_A^{\text{neq}}(t)$ is the non-equilibrium Massieu potential. This inequality indicates that the path from non-equilibrium to equilibrium has a lower bound on work. In engineering, the effective energy from non-equilibrium to equilibrium is referred to as **exergy**.⁷⁴ The non-equilibrium thermodynamic potential introduced here can be regarded as a generalization of it.

The difference between $(\tilde{W}_A^{\text{ext}})_{A \rightarrow n}$ and $-(\Delta\Phi_A^{\text{neq}})_{A \rightarrow n}$ corresponds to the entropy production defined as

$$(\Sigma_A)_{A \rightarrow n} = (\tilde{W}_A^{\text{ext}})_{A \rightarrow n} + (\Delta\Phi_A^{\text{neq}})_{A \rightarrow n} \geq 0. \quad (11)$$

For two non-equilibrium states A and B , we have $(\Sigma_A)_{A \rightarrow B} = (\Sigma_A)_{A \rightarrow n} - (\Sigma_A)_{B \rightarrow n}$. Thus, the entropy production rate for any non-equilibrium process at times t and $t+dt$ (where dt is an infinitesimal time) is expressed as

$$\frac{d\Sigma_A(t)}{dt} = \frac{d\tilde{W}_A^{\text{ext}}(t)}{dt} + \frac{d\Phi_A^{\text{neq}}(t)}{dt}. \quad (12)$$

As shown in Appendix B, the entropy production rate is always positive, i.e., $d\Sigma_A(t)/dt \geq 0$. Thus, we have the inequality $(\tilde{W}_A^{\text{ext}})_{A \rightarrow B}^{\text{min}} \geq -(\Delta\Phi_A^{\text{neq}})_{A \rightarrow B}$, or

$$\frac{d\tilde{W}_A^{\text{ext}}(t)}{dt} \geq -\frac{d\Phi_A^{\text{neq}}(t)}{dt}, \quad (13)$$

which we call **the DL non-equilibrium minimum work principle**. While $\tilde{W}_A^{\text{ext}}(t)$ and $\Sigma_A(t)$ are not state variables because they depend on a path, $\Phi_A^{\text{neq}}(t)$ is a state variable defined by the non-equilibrium-to-equilibrium minimum work path. When state B is on the non-equilibrium-to-equilibrium minimum work path from A to n , equality in Eq. (13) holds.

Using Eqs. (2) and (12), we obtain the time derivative form of the non-equilibrium Massieu potential as

$$\frac{d\Phi_A^{\text{neq}}(t)}{dt} = -U_A^{\text{neq}} \frac{d\beta(t)}{dt} - \tilde{x}(t) \frac{dX_A^{\text{neq}}(t)}{dt} + \frac{d\Sigma_A(t)}{dt}. \quad (14)$$

The convexity of DL potentials is discussed on the basis of the SB model in Appendix C. Thus, these can be regarded as thermodynamic potentials.

Using Eqs. (6), we have the non-equilibrium Planck potential expressed as

$$\frac{d\Xi_A^{\text{neq}}(t)}{dt} = -U_A^{\text{neq}} \frac{d\beta(t)}{dt} + X_A^{\text{neq}}(t) \frac{d\tilde{x}(t)}{dt} + \frac{d\Sigma_A(t)}{dt}. \quad (15)$$

The M-entropy $\Lambda_A^{\text{neq}}(t)$ and P-entropy $\Gamma_A^{\text{neq}}(t)$ can be evaluated from the TDL transformations (6) and (7). The non-equilibrium potentials satisfy the following Legendre transformations:

$$\Xi_A^{\text{neq}}(t) = \Phi_A^{\text{neq}}(t) + \tilde{x}(t)X_A^{\text{neq}}(t) \quad (16)$$

and

$$\Lambda_A^{\text{neq}}(t) = \Phi_A^{\text{neq}}(t) + \beta(t)U_A^{\text{neq}}(t). \quad (17)$$

The time derivative forms of the DL non-equilibrium entropic potentials are summarized in Table I. Note that the entropic potentials, the intensive variables, and the non-equilibrium extensive variables are state variables, whereas their time derivatives are not state variables.

As shown in Appendix D, the non-equilibrium Massieu potential is always smaller than the quasi-static Massieu potential. This indicates that the non-equilibrium Massieu potential is minimum when the state is equilibrium. In the quasi-static case, Table I is reduced to Table V (Appendix A). Thus, we can regard these potentials as extensions of the thermodynamic potentials to a non-equilibrium regime.

From Eqs. (12) and (17), the entropy production rate is expressed using the non-equilibrium M-entropy as

$$\frac{d\Sigma_A(t)}{dt} = \frac{d\Lambda_A^{\text{neq}}(t)}{dt} - \frac{d\tilde{Q}_A^{\text{ext}}(t)}{dt}. \quad (18)$$

2. Non-equilibrium Helmholtz–Gibbs potentials

We introduce non-equilibrium Helmholtz and Gibbs energies defined as $F_A^{\text{neq}}(t) = -\Phi_A^{\text{neq}}(t)/\beta(t)$ and $G_A^{\text{neq}}(t) = -\Xi_A^{\text{neq}}(t)/\beta(t)$. Because $d\beta(t)/dt = -(1/k_B T^2(t))dT(t)/dt$, we obtain the time derivative forms of these from Eqs. (14) and (15) as

$$\frac{dF_A^{\text{neq}}(t)}{dt} = -S_A^{\text{neq}}(t)\frac{dT(t)}{dt} + x(t)\frac{dX_A^{\text{neq}}(t)}{dt} + \frac{dQ_A^{\text{wst}}(t)}{dt} \quad (19)$$

and

$$\frac{dG_A^{\text{neq}}(t)}{dt} = -S_A^{\text{neq}}(t)\frac{dT(t)}{dt} - X_A^{\text{neq}}(t)\frac{dx(t)}{dt} + \frac{dQ_A^{\text{wst}}(t)}{dt}, \quad (20)$$

where $S_A^{\text{neq}}(t) = k_B\Lambda_A^{\text{neq}}(t)$ is a non-equilibrium entropy, and we have introduced the waste heat current as

$$\frac{dQ_A^{\text{wst}}(t)}{dt} = -\frac{1}{\beta(t)}\frac{d\Sigma_A(t)}{dt}. \quad (21)$$

From Eq. (16), we obtain the TDL transformation between the non-equilibrium Gibbs and Helmholtz potentials as

$$F_A^{\text{neq}}(t) = G_A^{\text{neq}}(t) + x(t)X_A^{\text{neq}}(t). \quad (22)$$

Solving Eq. (17) for $U_A^{\text{neq}}(t)$, yields the following TDL transformations:

$$U_A^{\text{neq}}(t) = F_A^{\text{neq}}(t) + T(t)S_A^{\text{neq}}(t). \quad (23)$$

From the above equations, we obtain the time derivative expressions for the enthalpy and internal energy. The results are summarized in Table II. These results are reduced to those in Table VI (Appendix A) for the quasi-static case. Thus, we can regard these potentials as extensions of thermodynamic potentials to a non-equilibrium regime.

Dividing both sides of Eq. (3) by $\beta(t)$ yields the first law of thermodynamics expressed for the internal energy as

$$\frac{dU_A^{\text{neq}}(t)}{dt} = \frac{dW_A^{\text{ext}}(t)}{dt} + \frac{dQ_A^{\text{ext}}(t)}{dt}, \quad (24)$$

where

$$\frac{dQ_A^{\text{ext}}(t)}{dt} = \frac{1}{\beta(t)}\frac{d\tilde{Q}_A^{\text{ext}}(t)}{dt} \quad (25)$$

is the extensive heat current. From Eqs. (18) and (25), we can evaluate the entropy production rate as

$$\frac{d\Sigma_A(t)}{dt} = \frac{1}{k_B} \left\{ \frac{dS_A^{\text{neq}}(t)}{dt} - \frac{1}{T(t)}\frac{dQ_A^{\text{ext}}(t)}{dt} \right\}. \quad (26)$$

In the isothermal case, by integrating both sides of the two equilibrium states over time t , we obtain^{28,58}

$$\Sigma_A(t) = \frac{1}{k_B} \left\{ \Delta S_A^{\text{qst}} - \frac{Q_A^{\text{ext}}}{T} \right\}. \quad (27)$$

The non-equilibrium Gibbs energy satisfies

$$S_A^{\text{neq}}(t) = - \left(\frac{\partial G_A^{\text{neq}}}{\partial T(t)} \right)_{x(t), \tilde{Q}^{\text{wst}}}, \quad (28)$$

$$X_A(t) = - \left(\frac{\partial G_A^{\text{neq}}}{\partial x(t)} \right)_{T(t), \tilde{Q}^{\text{wst}}}, \quad (29)$$

and

$$H_A(t) = -T^2(t)\frac{\partial}{\partial T(t)} \left(\frac{G_A^{\text{neq}}(t)}{T(t)} \right)_{x(t), \tilde{Q}^{\text{wst}}}. \quad (30)$$

Equation (30) extends the Gibbs–Helmholtz relation to a non-equilibrium regime.

III. NUMERICAL DEMONSTRATION

Although the results presented in Tables I and II hold for any non-equilibrium system consisting of subsystem and bath, the extensive variables and entropy production that appear in these relationships are system-specific, and there is no general theory on the basis of which non-equilibrium thermodynamic potentials can be obtained. However, it is possible to evaluate them as functions of intensive and extensive variables using an optimization algorithm. Here, as a demonstration, we evaluate non-equilibrium thermodynamic potentials numerically using the thermodynamic SB model.^{61,62}

TABLE I. Time derivative forms of the non-equilibrium (neq) Massieu–Planck potentials as functions of intensive variables $\beta(t)$ and $\tilde{x}(t)$ and extensive variables $U_A^{\text{neq}}(t)$ and $X_A^{\text{neq}}(t)$. Of the DL entropies, the commonly used one, which we call the Massieu entropy (M-entropy), involves only extensive variables and is denoted by $\Lambda_A^{\text{neq}}[U_A^{\text{neq}}(t), X_A^{\text{neq}}(t)]$, whereas the less widely used one, which we call the Planck entropy (P-entropy), is denoted by $\Gamma_A^{\text{qst}}[U_A^{\text{qst}}, \tilde{x}]$. Because heat is always lost in non-equilibrium processes, the entropy production rate $d\Sigma_A/dt$ appears in the equations. Each potential is related to others via Legendre transformations shown in the final column.

| neq DL Thermodynamic pot. | Differential Form | Natural var. | Legendre Transformation |
|---------------------------|---|--------------------------------------|--|
| Massieu | $\frac{d}{dt}\Phi_A^{\text{neq}} = -U_A^{\text{neq}}\frac{d}{dt}\beta - \tilde{x}\frac{d}{dt}X_A^{\text{neq}} + \frac{d}{dt}\Sigma_A$ | β, X_A^{neq} | \dots |
| Planck | $\frac{d}{dt}\Xi_A^{\text{neq}} = -U_A^{\text{neq}}\frac{d}{dt}\beta + X_A^{\text{neq}}\frac{d}{dt}\tilde{x} + \frac{d}{dt}\Sigma_A$ | β, \tilde{x} | $\Xi_A^{\text{neq}} = \Phi_A^{\text{neq}} + \tilde{x}X_A^{\text{neq}}$ |
| M-Entropy | $\frac{d}{dt}\Lambda_A^{\text{neq}} = \beta\frac{d}{dt}U_A^{\text{neq}} - \tilde{x}\frac{d}{dt}X_A^{\text{neq}} + \frac{d}{dt}\Sigma_A$ | $U_A^{\text{neq}}, X_A^{\text{neq}}$ | $\Lambda_A^{\text{neq}} = \Phi_A^{\text{neq}} + \beta U_A^{\text{neq}}$ |
| P-Entropy | $\frac{d}{dt}\Gamma_A^{\text{neq}} = \beta\frac{d}{dt}U_A^{\text{neq}} + X_A^{\text{neq}}\frac{d}{dt}\tilde{x} + \frac{d}{dt}\Sigma_A$ | $U_A^{\text{neq}}, \tilde{x}$ | $\Gamma_A^{\text{neq}} = \Lambda_A^{\text{neq}} + \tilde{x}X_A^{\text{neq}}$ |

TABLE II. Time derivative forms of the non-equilibrium (neq) Helmholtz–Gibbs potentials as functions of intensive variables $T(t)$ and $x(t)$ and extensive variables $S_A^{\text{neq}}(t)$ and $X_A^{\text{neq}}(t)$, which are interrelated through the Legendre transformations shown in the final column. Because heat is always lost in non-equilibrium processes, the waste heat Q_A^{wst} appears in the equations.

| neq Thermodynamic pot. | Differential Form | Natural var. | Legendre Transformation |
|------------------------|--|--------------------------------------|---|
| Helmholtz Energy | $\frac{d}{dt}F_A^{\text{neq}} = -S_A^{\text{neq}}\frac{d}{dt}T + x\frac{d}{dt}X_A^{\text{neq}} + \frac{d}{dt}Q_A^{\text{wst}}$ | T, X_A^{neq} | - |
| Gibbs Energy | $\frac{d}{dt}G_A^{\text{neq}} = -S_A^{\text{neq}}\frac{d}{dt}T - X_A^{\text{neq}}\frac{d}{dt}x + \frac{d}{dt}Q_A^{\text{wst}}$ | T, x | $G_A^{\text{neq}} = F_A^{\text{neq}} - xX_A^{\text{neq}}$ |
| Internal Energy | $\frac{d}{dt}U_A^{\text{neq}} = T\frac{d}{dt}S_A^{\text{neq}} + x\frac{d}{dt}X_A^{\text{neq}} + \frac{d}{dt}Q_A^{\text{wst}}$ | $S_A^{\text{neq}}, X_A^{\text{neq}}$ | $U_A^{\text{neq}} = F_A^{\text{neq}} + TS_A^{\text{neq}}$ |
| Enthalpy | $\frac{d}{dt}H_A^{\text{neq}} = T\frac{d}{dt}S_A^{\text{neq}} - X_A^{\text{neq}}\frac{d}{dt}x + \frac{d}{dt}Q_A^{\text{wst}}$ | S_A^{neq}, x | $H_A^{\text{neq}} = U_A^{\text{neq}} - xX_A^{\text{neq}}$ |

A. Thermodynamic system-bath model

We employed the Ullersma–Caldeira–Leggett (or Brownian) model,^{33–35,75–78} which is ideal for thermodynamic simulations because the subsystem and bath are well defined, and rigorous numerical solutions can be obtained in both classical and quantum cases under any time-dependent external perturbation. Many of the favorable features for thermodynamic investigations arise from the presence of a counter term, which allows us to include the contribution of the SB interactions in the bath.^{39–41,77–79}

By introducing multiple heat baths at different temperatures controlled by time-dependent SB coupling functions, we can investigate isothermal, isentropic, thermostatic, and entropic processes. The total Hamiltonian for isothermal and thermostatic processes is written as^{61,62}

$$\hat{H}_{\text{tot}}(t) = \hat{H}_A^0 + \hat{H}'_A(t) + \sum_{k=0}^N \hat{H}_{\text{IB}}^k(t), \quad (31)$$

where

$$\hat{H}_A^0 = \frac{\hat{p}^2}{2m} + U(\hat{q}) \quad (32)$$

is the unperturbed Hamiltonian of a subsystem with mass m and potential $U(\hat{q})$ described by momentum \hat{p} and position \hat{q} . The internal energy is then evaluated as $U_A^{\text{neq}}(t) = \text{tr}\{\hat{H}_A^0 \hat{\rho}_A(t)\}$, where $\hat{\rho}_A(t)$ is the reduced density operator of the subsystem. The external perturbation is expressed as $\hat{H}'_A(t) \equiv -x(t)\hat{X}_A$, where \hat{X}_A is an operator of the subsystem coordinate [i.e., $\hat{X}_A(\hat{q})$], and $x(t)$ is the thermodynamic intensive variable. The extensive variable is evaluated as $X_A^{\text{neq}}(t) = \text{tr}\{\hat{X}_A \hat{\rho}_A(t)\}$.

Although the conventional SB model has been limited to the investigation of isothermal processes at constant temperature, we can extend it to describe thermostatic processes in which temperature varies with time by introducing N independent heat baths, each in the thermal equilibrium state at the inverse temperature $\beta_k \equiv 1/k_B T_k$ connected to or disconnected from subsystem A using the window function $\xi_k(t)$.⁶¹ The k th bath Hamiltonian is expressed as an ensemble of harmonic oscillators and is given by

$$\hat{H}_{\text{IB}}^k(t) \equiv \sum_j \left\{ \frac{(\hat{p}_j^k)^2}{2m_j} + \frac{m_j^k (\omega_j^k)^2}{2} \left[\hat{x}_j^k - \frac{c_j^k A_k \xi_k(t) \hat{q}}{m_j^k (\omega_j^k)^2} \right]^2 \right\}, \quad (33)$$

where the momentum, position, mass, and frequency of the j th bath oscillator are given by \hat{p}_j^k , \hat{x}_j^k , m_j^k , and ω_j^k , respectively. Here, we consider the situation, in which N independent heat baths, each in the thermal equilibrium state $\exp(-\beta_k \hat{H}_{\text{IB}}^k)$ at the inverse temperature $\beta_k \equiv 1/k_B T_k$, are connected or disconnected to subsystem A according to a control function $\xi_k(t)$. The bath temperature can be effectively expressed as

$$T(t) = \sum_{k=1}^N T_k \xi_k(t), \quad (34)$$

or the inverse temperature as $\beta(t) = [k_B T(t)]^{-1}$. As a spectral distribution function of the k th bath $J^k(\omega) \equiv \sum_j \hbar (c_j^k A_k)^2 / (2m_j^k \omega_j^k) \delta(\omega - \omega_j^k)$, we consider the Ohmic case described by

$$J^k(\omega) = \frac{\hbar A_k^2 \omega}{\pi} \quad (35)$$

and assume that the time scale of quantum thermal fluctuations $\beta(t)\hbar/2\pi$ is shorter than the time scale of the external perturbations $\beta(t)$ and $x(t)$. This allows us to extend the low-temperature quantum Fokker-Planck equations (LT-QFPE)⁶⁶ for the set of Wigner distribution functions $W_{\vec{n}}(p, q; t)$, where \vec{n} is the index of hierarchy members, and the Kramers equation for the phase space distribution function $W(p, q; t)$ to the thermostatic case by introducing time-dependent Matsubara frequencies $\nu(t) = 1/\hbar\beta(t)$. The expressions for the thermodynamic quantum Fokker-Planck equations (T-QFPE) and thermodynamic Kramers equation (T-KE) are given in Refs. 61 and 62. The source codes for them are also provided in the supplementary material.⁶²

While the HEOM approach to thermodynamics treats the SB interaction as part of the main system in spin-boson systems,^{28–31,58–60} this Brownian model treats it as part of a heat bath, including the counter term.^{61,62} Assuming the Ohmic SDF, in the classical and high-temperature semi-classical cases, the dynamics described by this model exhibit a Markovian feature, which can be treated in the framework of stochastic thermodynamics, while in the fully quantum case, it is not only non-Markovian, but also non-factorized owing to bath-entanglement. In other words, the difference between the classical and quantum results represents a deviation from Markovian thermodynamics that arises when dealing with fully quantum processes.

It should be noted that for non-Markovian processes, the SDF-based description of a thermal bath breaks down when the correlation time of the noise is longer than the time scale of the bath temperature change.⁶² In such cases, prescriptions that simply replace β with $\beta(t)$ are not allowed, and the hierarchy members for each bath at different temperatures must be treated separately.⁶⁰ In this way, several baths can be operated simultaneously, although this is computationally expensive.^{30,31}

B. DL work and extensive variables

We express the solution for reduced density elements under any $x(t)$ in the Wigner representation using the zeroth member of the hierarchical Wigner functions as $W(p, q, t) \equiv W_{\vec{0}}(p, q; t)$. In the classical limit $\hbar \rightarrow 0$, $W(q, p; t)$ corresponds to the classical distribution function. We use this to define the change in DL intensive work over time, which corresponds to power and heat flow as follows:

$$\frac{d\tilde{W}_{\text{A}}^{\text{int}}(t)}{dt} = U_{\text{A}}^{\text{neq}}(t) \frac{d\beta(t)}{dt} - X_{\text{A}}^{\text{neq}}(t) \frac{d\tilde{x}(t)}{dt}, \quad (36)$$

where the extensive variables in the Wigner representation at time t are expressed as

$$X_{\text{A}}^{\text{neq}}(t) = \text{tr}_{\text{A}}\{X_{\text{A}}(q)W(p, q; t)\} \quad (37)$$

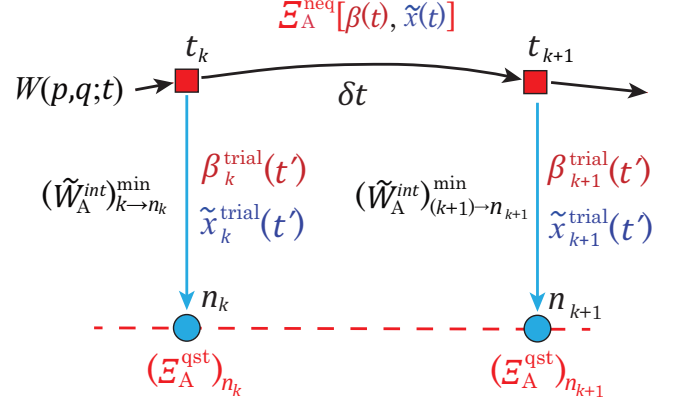


FIG. 1. Schematic of the evaluation of the non-equilibrium Planck potential $\Xi_{\text{A}}^{\text{neq}}(t)$ at t_k and t_{k+1} . A non-equilibrium process driven by the intensive variables $\beta(t)$ and $\tilde{x}(t)$ is described as the non-equilibrium distribution $W(p, q; t)$ expressed by the black arrows. The equilibrium states for different sets of β^{qst} and \tilde{x}^{qst} are expressed by the red dashed line. For each state k to the equilibrium state n_k , we minimize $(\tilde{W}_{\text{A}}^{\text{int}})_{k \rightarrow n_k}^{\text{min}} + (\Xi_{\text{A}}^{\text{qst}})_{n_k}$ by choosing the trial functions $\beta_k^{\text{trial}}(t')$ and $\tilde{x}_k^{\text{trial}}(t')$, where $(\tilde{W}_{\text{A}}^{\text{int}})_{k \rightarrow n_k}^{\text{min}}$ is the DL minimum intensive work for $k \rightarrow n_k$ and $(\Xi_{\text{A}}^{\text{qst}})_{n_k}$ is the quasi-static Planck potential at the state n_k . We can then evaluate the non-equilibrium Planck potential at state k as $(\Xi_{\text{A}}^{\text{neq}})_k = (\tilde{W}_{\text{A}}^{\text{int}})_{k \rightarrow n_k}^{\text{min}} + (\Xi_{\text{A}}^{\text{neq}})_{n_k}$.

and

$$U_{\text{A}}^{\text{neq}}(t) = \text{tr}_{\text{A}} \left\{ \left[\frac{p^2}{2m} + U(q) \right] W(p, q; t) \right\}. \quad (38)$$

From the definition (2) of extensive work and the TDL transformations (6) and (7), the extensive heat current can be evaluated as

$$\frac{dQ_{\text{A}}^{\text{ext}}(t)}{dt} = \text{tr}_{\text{A}} \left\{ \left[\frac{p^2}{2m} + U(q) - x(t)X_{\text{A}}(q) \right] \frac{\partial W(p, q; t)}{\partial t} \right\}. \quad (39)$$

C. Evaluation of the non-equilibrium Planck potential

From Eq. (B1), we obtain the following expression for the non-equilibrium Planck potential $(\Xi_{\text{A}}^{\text{neq}})_k = \Xi_{\text{A}}^{\text{neq}}[\beta(t_k), \tilde{x}(t_k)]$ of the non-equilibrium-to-equilibrium process $k \rightarrow n_k$ as

$$(\Xi_{\text{A}}^{\text{neq}})_k = (\tilde{W}_{\text{A}}^{\text{int}})_{k \rightarrow n_k}^{\text{min}} + (\Xi_{\text{A}}^{\text{qst}})_{n_k}, \quad (40)$$

where n_k represents the equilibrium state, $(\tilde{W}_{\text{A}}^{\text{int}})_{k \rightarrow n_k}^{\text{min}}$ is the DL minimum intensive work for $k \rightarrow n_k$, and $(\Xi_{\text{A}}^{\text{qst}})_{n_k}$ is the quasi-static Planck potential at state n_k . As shown in Eq. (B5), the right-hand side of Eq. (40) is independent

of the choice of n_k ; thus, to evaluate $(\Xi_A^{\text{neq}})_k$, we do not specify n_k to minimize $(\tilde{W}_A^{\text{int}})_{k \rightarrow n_k} + (\Xi_A^{\text{qst}})_{n_k}$.

To perform numerical calculations, we express Eq. (40) with Eq. (15) in terms of trial functionals $\beta^{\text{trial}}(t_k, t')$ and $\tilde{x}^{\text{trial}}(t_k, t')$ as

$$X_A^{\text{target}}[\beta^{\text{trial}}(t), x^{\text{trial}}(t)] = \Xi_A^{\text{qst}}(\beta_{n_k}^{\text{qst}}, x_{n_k}^{\text{qst}}) + \int_t^{t+\Delta t} \left[U_A(t') \frac{d\beta^{\text{trial}}(t')}{dt'} - X_A(t') \frac{d\tilde{x}^{\text{trial}}(t')}{dt'} \right] dt', \quad (41)$$

where $\Xi_A^{\text{target}}[\beta^{\text{trial}}(t), \tilde{x}^{\text{trial}}(t)]$ is the target function to be minimized and $\Xi_A^{\text{qst}}(\beta_{n_k}^{\text{qst}}, \tilde{x}_{n_k}^{\text{qst}})$ is the quasi-static Planck potential at n_k , which is also evaluated from the T-QFPE and T-KE. The DL trial functional $\tilde{x}_k^{\text{trial}}(t)$ in Eq. (41) is evaluated from $x_k^{\text{trial}}(t)$ as $\tilde{x}_k^{\text{trial}}(t) = \beta_k^{\text{trial}}(t)x_k^{\text{trial}}(t)$. To reduce computational cost, we assume that the optimized trial functionals are constant after the characteristic time for the equilibration Δt , as $\beta_k^{\text{trial}}(t_k + \Delta t) = \beta_{n_k}^{\text{qst}}$ and $x_k^{\text{trial}}(t_k + \Delta t) = x_{n_k}^{\text{qst}}$.

As trial functionals for time $t' > t_k$, we chose the N_β th and N_x th Taylor expansion forms expressed as

$$\beta_k^{\text{trial}}(t') = \sum_{n=0}^{N_\beta} \beta_k^{(n)}(t' - t_k)^n, \quad (42)$$

and

$$x_k^{\text{trial}}(t') = \sum_{n=0}^{N_x} x_k^{(n)}(t' - t_k)^n, \quad (43)$$

where $\beta_k^{(n)}$ and $x_k^{(n)}$ are the n th-order Taylor coefficients. Thus, the functional minimization of $\Xi_A^{\text{target}}[\beta^{\text{trial}}(t), \tilde{x}^{\text{trial}}(t)]$ becomes a multivariable functional minimization for $\beta_k^{(n)}$ and $x_k^{(n)}$.

Then, $\Xi_A^{\text{neq}}(t)$ is evaluated as follows (see Fig. 1). First, we perform the non-equilibrium simulations for given $\beta(t)$ and $\tilde{x}(t)$ to obtain $W_{\tilde{n}}(p, q; t)$ for each t_k . The minimum work from the non-equilibrium state k to the equilibrium state n_k expressed as $(\tilde{W}_A^{\text{int}})_{k \rightarrow n_k}^{\text{min}}$ is then evaluated by an optimization algorithm for $\beta_k^{\text{trial}}(t')$ and $\tilde{x}_k^{\text{trial}}(t')$. From Eq. (40), we set this value as $(\Xi_A^{\text{neq}})_k$. By repeating this procedure for different k values, we obtain $\Xi_A^{\text{neq}}(t_k)$ at each step. The other potentials can be evaluated by using the TDL transformations.

D. Thermostatic quantum and classical Stirling engines

The non-equilibrium thermodynamic potentials are state variables as functions of the non-equilibrium intensive and extensive variables, which are also state variables, whereas Q_A^{wst} is not; in the quasi-static limit, they reduce to conventional thermodynamic potentials. These non-equilibrium potentials are useful because they can be used to analyze thermodynamic processes using work diagrams, as in the case of equilibrium thermodynamics.

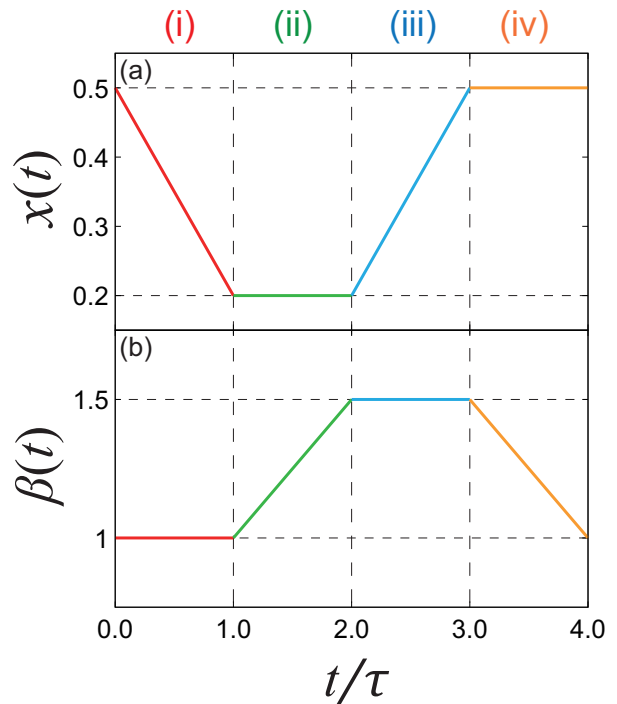


FIG. 2. Time profiles of (a) the electric field $x(t)$ and (b) the inverse temperature $\beta(t)$ for the thermostatic Stirling engine. The red, green, blue, and orange lines represent (i) hot isothermal, (ii) isoelectric (hot to cold), (iii) cold isothermal, and (iv) isoelectric (cold to hot) processes, respectively.⁶² The time t is normalized by the period of the cycle τ .

By identifying a thermodynamic process that minimizes entropy production, we can construct a heat machine with maximum efficiency under non-equilibrium conditions, although the efficiency is lower than the Carnot limit.^{58,59}

Here, we demonstrate how to evaluate non-equilibrium potentials for the case in which $\beta(t)$ and $x(t)$ are specified. For this purpose, we consider a thermostatic classical/quantum Stirling engine⁶² consisting of four steps: (i) a hot isothermal process, (ii) a transition from a hot-to-cold thermostatic process, (iii) a cold isothermal process, and (iv) a transition from a cold-to-hot thermostatic process for an anharmonic potential system. Since the purpose of the calculation is to illustrate how potentials are calculated, we fix the changes in $\beta(t)$ and $x(t)$ as shown in Fig. 2 with $\tau = 20$ and do not optimize them to improve their efficiency.

1. Simulation details

We performed simulations using the anharmonic potential system employed in our previous studies.^{61,62} Thus, we considered a quartic anharmonic potential with the external interaction described as $X_A(\hat{q}) = \hat{q}$. The po-

TABLE III. Parameter values used for the simulations of the thermostatic Stirling engine. Here, dx and dp are the mesh sizes for position and momentum, respectively, in Wigner space. The integers N and K are the cutoff numbers used in the T-QFPE.

| | A | N | K | dx | dp |
|-----------|---------|-----|-----|------|------|
| Classical | 0.5–1.5 | ... | ... | 0.25 | 0.25 |
| Quantum | 0.5 | 6 | 2 | 0.3 | 0.4 |
| | 1.0 | 7 | 2 | 0.3 | 0.5 |
| | 1.5 | 8 | 2 | 0.3 | 0.6 |

TABLE IV. Work performed in one cycle for the classical and quantum cases for different SB coupling strengths.

| A | W (classical) | W (quantum) |
|--------------------|------------------------|------------------------|
| 0.5 (weak) | -1.44×10^{-2} | -1.07×10^{-2} |
| 1.0 (intermediate) | -5.77×10^{-3} | -3.09×10^{-3} |
| 1.5 (strong) | 1.01×10^{-2} | 1.10×10^{-2} |

tential function in Eq. (32) is expressed as

$$U(\hat{q}) = U_2 \hat{q}^2 + U_3 \hat{q}^3 + U_4 \hat{q}^4, \quad (44)$$

where the constants are given by $U_2 = 0.1$, $U_3 = 0.02$, and $U_4 = 0.05$. Numerical calculations were performed to integrate the T-QFPE in the quantum cases and the T-KE in the classical cases. The detailed conditions for the numerical calculations, including the working parameters, are presented in Table III and in Ref. 61. Source code and results for the quasi-static case are presented in Ref. 62.

To set the trial functions defined in Eqs. (42) and (43), we chose $N_\beta = N_x = 5$. Then, using the Nelder–Mead method, we minimized $\Xi_A^{\text{target}}[\beta^{\text{trial}}(t), x^{\text{trial}}(t)]$ in Eq. (41) with a cutoff time $\Delta t = 1.0$. We evaluated $\Xi_A^{\text{neq}}(t)$ in 20 steps. The value of the quasi-static Planck potential $\Xi_A^{\text{qst}}(\beta^{\text{qst}}, \tilde{x}^{\text{qst}})$ in Eq. (41) was obtained by integrating the thermodynamic T-QFPE and the T-KE.

2. Results

Extensive variables $X_A^{\text{neq}}(t)$ and $U_A^{\text{neq}}(t)$ were obtained from Eqs. (37) and (38), respectively. The non-equilibrium entropy expressed as $S_A^{\text{neq}}(t) = k_B \Lambda_A^{\text{neq}}(t)$ was then obtained from $X_A^{\text{neq}}(t)$, and $U_A^{\text{neq}}(t)$ and $\Xi_A^{\text{neq}}(t)$ were evaluated according to the procedure described in Sec. III C using the TDL transformations given by Eqs. (16) and (17). The results are depicted as non-equilibrium $x(t)$ – $X_A^{\text{neq}}(t)$ and $T(t)$ – $S_A^{\text{neq}}(t)$ diagrams, whose cycle trajectories are closed because the cycle is stationary and because $T(t)$, $S_A^{\text{neq}}(t)$, $x(t)$, and $X_A^{\text{neq}}(t)$ are state variables.

We first present the $x(t)$ – $X_A^{\text{neq}}(t)$ diagrams for weak ($A = 0.5$), intermediate ($A = 1.0$), and strong ($A = 1.5$)

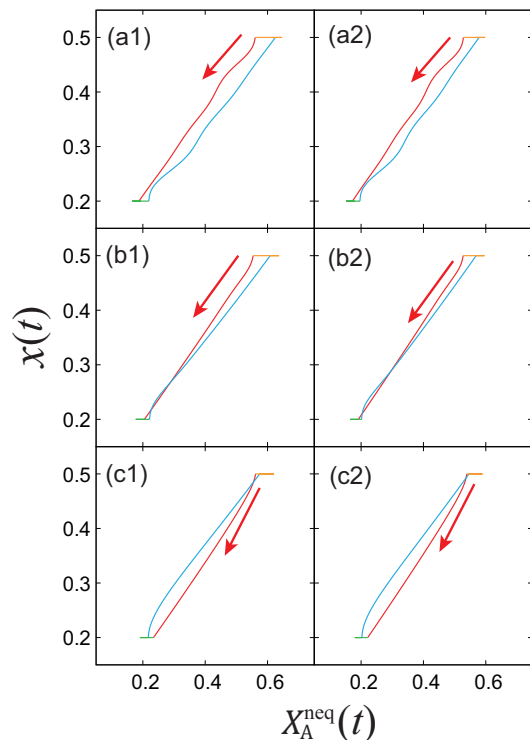


FIG. 3. $x(t)$ – $X_A^{\text{neq}}(t)$ diagrams for the thermostatic Stirling engine in the classical case (1, left column) and quantum case (2, right column) for (a) $A = 0.5$ (weak), (b) 1.0 (intermediate), and (c) 1.5 (strong) SB coupling strengths. In each plot, the four curves (or lines) represent (i) hot isothermal (red), (ii) hot to cold thermostatic (green), (iii) cold isothermal (blue), and (iv) cold to hot thermostatic (orange) processes, respectively. These processes evolve in a counterclockwise manner over time in a heat engine, whereas they evolve in a clockwise manner over time in a refrigerator.

SB coupling strengths in Fig. 3. The results for the quasi-static case are presented in Fig. 5 in Ref. 62.

The area enclosed by each diagram corresponds to positive work when evolving in the counterclockwise direction, whereas negative work corresponds to clockwise evolution. The work performed in one cycle is presented in Table IV. In each diagram in Fig. 3, the red and blue horizontal lines appear because a time delay exists in the change of $X_A^{\text{neq}}(t)$ with respect to $x(t)$ for the heat bath to take effect.

As shown in Fig. 3 and Table IV, the larger the SB coupling, the smaller the quantum effect because it is suppressed by relaxation.⁶⁶ Thus, when the coupling is large, dissipation dominates, and the system becomes a refrigerator (or damper). This is because the time scales of fluctuation and dissipation are different: in the non-equilibrium case, dissipation dominates when SB coupling is large, whereas in the quasi-static case (Fig. 5 in Ref. 62), fluctuations and dissipation are balanced regardless of the coupling strength. This is a distinct difference from the

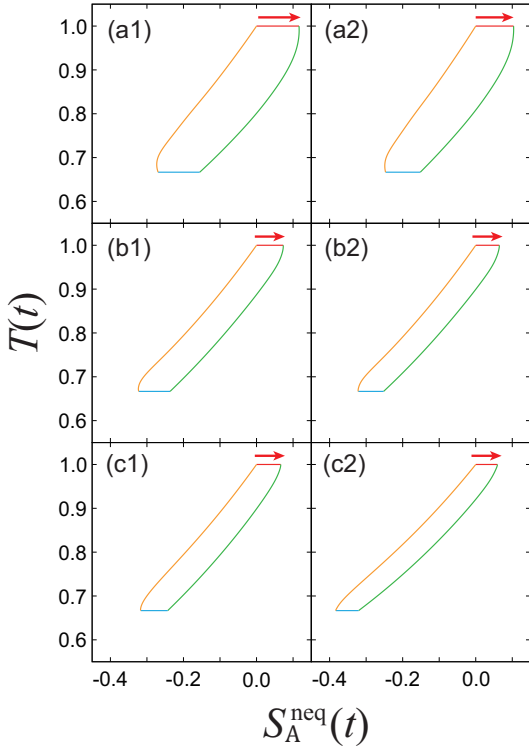


FIG. 4. $T(t)$ - $S_A^{\text{neq}}(t)$ diagrams for the thermostatic Stirling engine in the classical case (1, left column) and quantum case (2, right column) for (a) $A = 0.5$ (weak), (b) 1.0 (intermediate), and (c) 1.5 (strong) SB coupling strengths, respectively. Each cycle starts with a red arrow, and the four curves represent (i) hot isothermal (red), (ii) from hot to cold thermostatic (green), (iii) cold isothermal (blue), and (iv) from cold to hot thermostatic (orange) processes, respectively.

Carnot case; the efficiency reaches a maximum in the intermediate SB coupling region, where A is neither large nor small.⁵⁹

Next, we present the $T(t)$ - $S_A^{\text{neq}}(t)$ diagrams in Fig. 4. The results for the quasi-static case are presented in Fig. 6 in Ref. 62. The area enclosed by the clockwise curve represents the difference between the extensive heat and waste heat, $Q_A^{\text{ext}} - Q_A^{\text{wst}}$, per cycle. In the quasi-static case (Fig. 6 in Ref. 62), the area agree with the extensive heat per cycle because Q^{wst} becomes zero. In the thermostatic processes (green and orange curves), when SB coupling is small, a time delay is observed in the change in $S_A^{\text{neq}}(t)$ with respect to $T(t)$. This occurs because it takes time for the system to be excited when thermal fluctuations are small, whereas the delay is almost negligible when SB coupling is strong.

In Fig. 5, we show the (time-averaged) entropy production rate, enthalpy, and internal energy as functions of t . As we show in Sec. II, the entropy production rate is always positive, and becomes large in the isothermal case for larger SB coupling because of strong dissipation, whereas it becomes small in the thermostatic processes

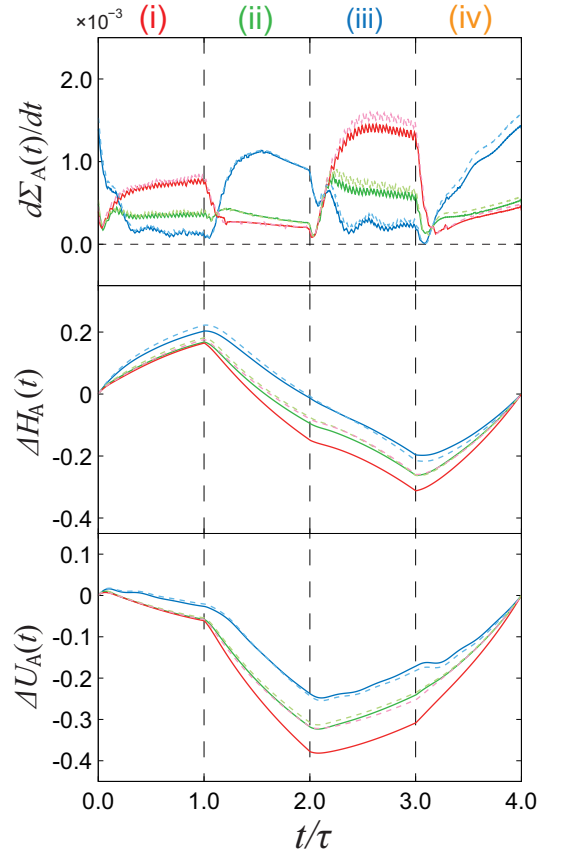


FIG. 5. (a) Entropy production rate $d\Sigma_A(t)/dt$, (b) the change of enthalpy $\Delta H_A(t)$, and (c) internal energy $\Delta U_A(t)$, as functions of t . The blue, green, and red curves represent the weak ($A = 0.5$), intermediate ($A = 1.0$), and strong ($A = 1.5$) SB coupling cases, respectively. The solid and dashed curves represent the quantum and classical results, respectively. The plots of the entropy production rate were time-averaged over 21 steps each using the raw data.

for the case of weak SB coupling because fluctuations are suppressed.

Using the graph of the entropy production rate, we can improve the cycle efficiency. For instance, in the case of strong coupling, because a large entropy production rate occurs in isothermal processes, increasing the duration of the isothermal processes reduces the entropy production in the cycle.

For weak SB coupling, both the enthalpy and internal energy in the classical case agree with those in the quantum case, whereas for strong SB coupling, they disagree because of bathentanglement.⁴⁰

IV. CONCLUSIONS

The virtue of thermodynamics lies in its ability to describe, in a system-independent manner, macroscopic thermal phenomena resulting from complex microscopic interactions as changes in thermodynamic potentials that

are described as interrelated intensive and extensive variables via Legendre transformations.

We developed the laws of thermodynamics as applied to work in a system-independent manner, based on the principle of DL minimum work. Subsequently, we have developed a non-equilibrium thermodynamic theory that describes the non-equilibrium Massieu–Planck potentials and Helmholtz–Gibbs potentials in time derivative form in terms of non-equilibrium extensive and intensive variables, which are state variables along with entropy production, which is not a state variable. Our results are summarized in Tables I and II and are consistent with traditional thermodynamics in a quasi-static case, as presented in Tables V and VI.

These results have been validated for thermostatic quantum and classical Stirling engines through numerical simulations based on the thermodynamic SB model, which can describe both isothermal and thermostatic processes. An optimization algorithm was used to evaluate non-equilibrium thermodynamic potentials. Work diagrams in non-equilibrium regimes were presented and analyzed.

In this paper, to perform numerical calculations, the external field was chosen as the intensive variable and the polarization as the extensive variable. In a Brownian model defined by a potential function, it is also possible to select pressure and volume as intensive and extensive variables, as the partition function was evaluated for an ideal gas.

Although our theory in the non-equilibrium regime is model-specific, it is possible to test it even in real systems by using optimization algorithms. By designing processes to reduce entropy production, efficient heat engines can be developed for non-equilibrium processes.

In engineering, the effective energy from non-equilibrium to equilibrium is referred to as exergy.⁷⁴ The non-equilibrium thermodynamic potentials introduced can be regarded as a generalization of this concept. This theory provides a methodology to systematically evaluate and improve it, which should be useful from the perspective of Sustainable Development Goals (SDGs).

ACKNOWLEDGMENTS

The authors thank Yoshi Oono for his critical comments on the definition and terminology of thermodynamic variables, particularly extensive variables. Y.T. was supported by JSPS KAKENHI (Grant No. B21H01884). S.K. was supported by a JST fellowship, the establishment of university fellowships towards the creation of science technology innovation (Grant No. JPMJFS2123), and by Grant-in-Aid for JSPS Fellows (Grant No. 24KJ1373).

AUTHOR DECLARATIONS

Conflict of Interest

The authors have no conflicts to disclose.

AUTHOR CONTRIBUTIONS

Shoki Koyanagi: Formal analysis (lead); Investigation (equal); Methodology (equal); Software (lead); Writing - original draft (equal). **Yoshitaka Tanimura:** Conceptualization (lead); Formal analysis (supporting); Funding acquisition (lead); Investigation (equal); Methodology (equal); Writing - review and editing (lead).

DATA AVAILABILITY

The data that support the findings of this study are available from the corresponding authors upon reasonable request.

Appendix A: Quasi-static thermodynamic potentials

We introduce the DL intensive heat defined as

$$\frac{d\tilde{Q}_A^{int}(t)}{dt} \equiv \beta(t) \frac{dU_A(t)}{dt} + X_A(t) \frac{d\tilde{x}(t)}{dt}, \quad (\text{A1})$$

which satisfies the Legendre transformation

$$\frac{d\tilde{Q}_A^{int}(t)}{dt} = \frac{d\tilde{Q}_A^{ext}(t)}{dt} + \frac{d}{dt} [\tilde{x}(t)X_A(t)]. \quad (\text{A2})$$

Extensive and intensive work and heat $\tilde{W}_A^{ext}(t)$, $\tilde{W}_A^{int}(t)$, $\tilde{Q}_A^{ext}(t)$, and $\tilde{Q}_A^{int}(t)$ are interrelated via Legendre transformations (6), (7), and (A2). Therefore, we obtain the inequalities (8), (9),

$$\tilde{W}_A^{int} \geq -\Delta \Xi_A^{qst}, \quad (\text{A3})$$

and

$$\tilde{Q}_A^{int} \leq \Delta \Gamma_A^{qst}, \quad (\text{A4})$$

where Γ_A^{qst} is the Planck entropy (P-entropy). These are all expressions of the second law of thermodynamics. The total differential forms of the Massieu–Planck potentials are presented in Table V.

The Helmholtz–Gibbs potentials can be obtained from the Massieu–Planck potentials using the definitions $F_A^{qst}(t) = -\Phi_A^{qst}(t)/\beta^{qst}(t)$ and $G_A^{qst}(t) = -\Xi_A^{qst}(t)/\beta^{qst}(t)$. From Eq. (6), we obtain

$$F_A^{qst}(t) = G_A^{qst}(t) + x^{qst}(t)X_A^{qst}(t). \quad (\text{A5})$$

TABLE V. Total differential expressions for the quasi-static (qst.) entropic potentials as functions of the intensive variables $\beta^{\text{qst}}(t)$ and $\tilde{x}^{\text{qst}}(t)$ and the extensive variables $U_A^{\text{qst}}(t)$ and $X_A^{\text{qst}}(t)$. Entropy has two definitions, depending on whether the work variable is intensive or extensive. Of these DL entropies, the commonly used one, which we call Massieu entropy (M-entropy), involves only extensive variables and is denoted by $\Lambda_A^{\text{qst}}[U_A^{\text{qst}}, X_A^{\text{qst}}]$, whereas the less widely used one, which we call Planck entropy (P-entropy), is denoted by $\Gamma_A^{\text{qst}}[U_A^{\text{qst}}, \tilde{x}^{\text{qst}}]$. Whereas the enthalpy $H_A^{\text{qst}}(t)$ was chosen as the natural variable in Ref. 61, here we chose the internal energy U_A^{qst} instead. Each potential is related to the others by the Legendre transformations shown in the final column.

| Qst. Potential | Differential form | Natural var. | Legendre transformation |
|----------------|---|--|--|
| Massieu | $d\Phi_A^{\text{qst}} = -U_A^{\text{qst}} d\beta^{\text{qst}} - \tilde{x}^{\text{qst}} dX_A^{\text{qst}}$ | $\beta^{\text{qst}}, X_A^{\text{qst}}$ | \dots |
| Planck | $d\Xi_A^{\text{qst}} = -U_A^{\text{qst}} d\beta^{\text{qst}} + X_A^{\text{qst}} d\tilde{x}^{\text{qst}}$ | $\beta^{\text{qst}}, \tilde{x}^{\text{qst}}$ | $\Xi_A^{\text{qst}} = \Phi_A^{\text{qst}} + \tilde{x}^{\text{qst}} X_A^{\text{qst}}$ |
| M-Entropy | $d\Lambda_A^{\text{qst}} = \beta^{\text{qst}} dU_A^{\text{qst}} - \tilde{x}^{\text{qst}} dX_A^{\text{qst}}$ | $U_A^{\text{qst}}, X_A^{\text{qst}}$ | $\Lambda_A^{\text{qst}} = \Xi_A^{\text{qst}} + \beta^{\text{qst}} U_A^{\text{qst}}$ |
| P-Entropy | $d\Gamma_A^{\text{qst}} = \beta^{\text{qst}} dU_A^{\text{qst}} + X_A^{\text{qst}} d\tilde{x}^{\text{qst}}$ | $U_A^{\text{qst}}, \tilde{x}^{\text{qst}}$ | $\Gamma_A^{\text{qst}} = \Phi_A^{\text{qst}} + \beta^{\text{qst}} U_A^{\text{qst}}$ |

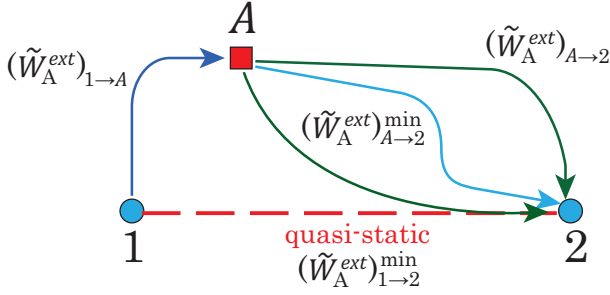


FIG. 6. Schematic to derive Eq. (B1). The blue circles 1 and 2 represent the equilibrium states, and the red square A represents the non-equilibrium state. The quasi-static work performed for $1 \rightarrow 2$ (red dashed line) is denoted by $(\tilde{W}_A^{\text{ext}})^{\text{min}}_{1 \rightarrow 2}$, while the non-equilibrium work from 1 to A (dark blue curve) is denoted by $(\tilde{W}_A^{\text{ext}})_{1 \rightarrow A}$. When $(\tilde{W}_A^{\text{ext}})_{1 \rightarrow A}$ is fixed, the value of $(\tilde{W}_A^{\text{ext}})_{A \rightarrow 2}$ depends on the path (green and light blue curves). From the second law of thermodynamics, we have $(\tilde{W}_A^{\text{ext}})_{1 \rightarrow A} + (\tilde{W}_A^{\text{ext}})_{A \rightarrow 2} \geq -(\Delta\Phi_A^{\text{qst}})_{1 \rightarrow 2}$. This indicates a lower bound of work for $A \rightarrow 2$ denoted by $(\tilde{W}_A^{\text{ext}})^{\text{min}}_{A \rightarrow 2}$ (light blue curve) and given by Eq. (B1).

Accordingly, from Eq. (7), we have

$$U_A^{\text{qst}}(t) = F_A^{\text{qst}}(t) + T^{\text{qst}}(t)S_A^{\text{qst}}(t), \quad (\text{A6})$$

where we have used $d\beta^{\text{qst}}(t)/dt = -(1/k_B[T^{\text{qst}}(t)]^2)dT^{\text{qst}}(t)/dt$ and $S_A^{\text{qst}}(t) = k_B\Lambda_A^{\text{qst}}(t)$.

The total differential forms of the Helmholtz–Gibbs potentials are presented in Table VI.

Appendix B: DL non-equilibrium minimum work principle

Here, we derive fundamental equations to develop the DL non-equilibrium minimum work principle. Consider two equilibrium states 1 and 2, which are connected by a quasi-static process (see Fig. 6). From the principle of DL minimum work [Eq. (8)], the work performed in this process is equivalent to the difference in the Massieu potentials: $(\tilde{W}_A^{\text{ext}})^{\text{min}}_{1 \rightarrow 2} = -(\Delta\Phi_A^{\text{qst}})_{1 \rightarrow 2} \equiv (\Phi_A^{\text{qst}})_1 - (\Phi_A^{\text{qst}})_2$, where $n \rightarrow n'$ represents the transition from any state n to n' . Separately, we consider the non-equilibrium state

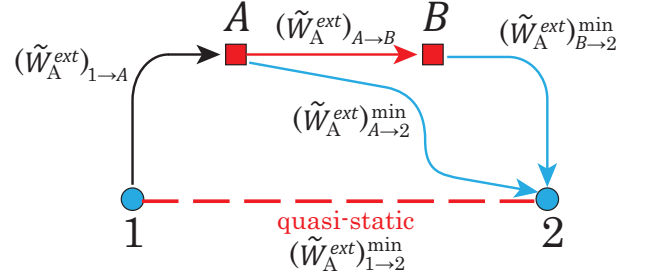


FIG. 7. Schematic for deriving the principle of DL non-equilibrium minimum work expressed by Eq. (B3). We consider two non-equilibrium states A and B (red square) that are connected by a non-equilibrium process described by the red arrow for $A \rightarrow B$. The light blue curves $A \rightarrow 2$ and $B \rightarrow 2$ represent non-equilibrium-to-equilibrium minimum work paths, whose work is denoted by $(\tilde{W}_A^{\text{ext}})^{\text{min}}_{A \rightarrow 2}$ and $(\tilde{W}_A^{\text{ext}})^{\text{min}}_{B \rightarrow 2}$, respectively.

A and introduce the non-equilibrium process $1 \rightarrow A$ (dark blue curve in Fig. 6), and any process from A to 2 (green and light blue curves). For each of these processes, the work performed is denoted by $(\tilde{W}_A^{\text{ext}})_{1 \rightarrow A}$ and $(\tilde{W}_A^{\text{ext}})_{A \rightarrow 2}$, respectively. For fixed $(\tilde{W}_A^{\text{ext}})_{1 \rightarrow A}$, the value of $(\tilde{W}_A^{\text{ext}})_{A \rightarrow 2}$ changes depending on path.

From the second law of thermodynamics [Eq. (8)], we obtain $(\tilde{W}_A^{\text{ext}})_{1 \rightarrow A} + (\tilde{W}_A^{\text{ext}})_{A \rightarrow 2} > -(\Delta\Phi_A^{\text{qst}})_{1 \rightarrow 2}$. This indicates that $(\tilde{W}_A^{\text{ext}})_{A \rightarrow 2}$ has a lower bound for fixed $(\tilde{W}_A^{\text{ext}})_{1 \rightarrow A}$; otherwise, the inequality is violated, for example, as follows: $-\infty > -(\Delta\Phi_A^{\text{qst}})_{1 \rightarrow 2} - (\tilde{W}_A^{\text{ext}})_{1 \rightarrow A}$. Using the lower bound of this work, we introduce the non-equilibrium Massieu potential Φ_A^{neq} defined as

$$(\tilde{W}_A^{\text{ext}})^{\text{min}}_{A \rightarrow 2} = -[(\Phi_A^{\text{qst}})_2 - (\Phi_A^{\text{neq}})_A]. \quad (\text{B1})$$

By introducing a second non-equilibrium state B on the pathway $A \rightarrow 2$ as depicted in Fig. 7, we now discuss the non-equilibrium transition $A \rightarrow B$ (red arrow). We consider the non-equilibrium-to-equilibrium minimum work from B to 2 (light blue curve), expressed as

$$(\tilde{W}_A^{\text{ext}})^{\text{min}}_{B \rightarrow 2} = -[(\Phi_A^{\text{qst}})_2 - (\Phi_A^{\text{neq}})_B]. \quad (\text{B2})$$

TABLE VI. Total differential expressions for the quasi-static (qst.) thermodynamic potentials as functions of intensive variables $T^{\text{qst}}(t)$ and $x^{\text{qst}}(t)$ and extensive variables $S_A^{\text{qst}}(t)$ and $X_A^{\text{qst}}(t)$. The potentials are related through the Legendre transformations shown in the final column

| Qst. potential | Differential form | Natural var. | Legendre transformation |
|----------------|--|--------------------------------------|---|
| Helmholtz | $dF_A^{\text{qst}} = -S_A^{\text{qst}} dT^{\text{qst}} + x^{\text{qst}} dX_A^{\text{qst}}$ | $T^{\text{qst}}, X_A^{\text{qst}}$ | \dots |
| Gibbs | $dG_A^{\text{qst}} = -S_A^{\text{qst}} dT^{\text{qst}} - X_A^{\text{qst}} dx^{\text{qst}}$ | $T^{\text{qst}}, x^{\text{qst}}$ | $G_A^{\text{qst}} = F_A^{\text{qst}} - x^{\text{qst}} X_A^{\text{qst}}$ |
| Internal | $dU_A^{\text{qst}} = T^{\text{qst}} dS_A^{\text{qst}} + x^{\text{qst}} dX_A^{\text{qst}}$ | $S_A^{\text{qst}}, X_A^{\text{qst}}$ | $U_A^{\text{qst}} = F_A^{\text{qst}} + T^{\text{qst}} S_A^{\text{qst}}$ |
| Enthalpy | $dH_A^{\text{qst}} = T^{\text{qst}} dS_A^{\text{qst}} - X_A^{\text{qst}} dx^{\text{qst}}$ | $S_A^{\text{qst}}, x^{\text{qst}}$ | $H_A^{\text{qst}} = G_A^{\text{qst}} + T^{\text{qst}} S_A^{\text{qst}}$ |

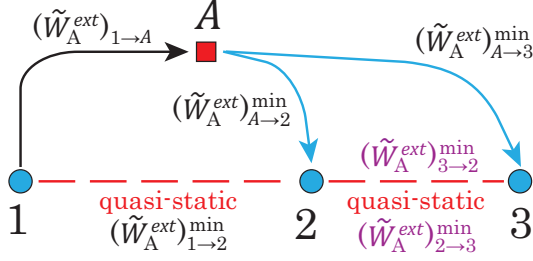


FIG. 8. Schematic showing that the non-equilibrium Massieu potential can be evaluated from any equilibrium state 3 instead of 2. To illustrate this, we consider the non-equilibrium-to-equilibrium path $A \rightarrow 3$, where we introduce a third equilibrium state denoted by 3 (blue circle). The work between the two equilibrium states is denoted by $(W_A^{\text{ext}})_{2 \rightarrow 3}^{\text{qst}}$ and $(W_A^{\text{ext}})_{3 \rightarrow 2}^{\text{qst}}$, respectively.

From the inequality $(\tilde{W}_A^{\text{ext}})_{A \rightarrow 2} \geq -[(\Phi_A^{\text{qst}})_2 - (\Phi_A^{\text{neq}})_A]$ and Eq. (B2), we obtain

$$(\tilde{W}_A^{\text{ext}})_{A \rightarrow B} \geq -(\Delta \Phi_A^{\text{neq}})_{A \rightarrow B}, \quad (\text{B3})$$

where $(\tilde{W}_A^{\text{ext}})_{A \rightarrow B} \equiv (\tilde{W}_A^{\text{ext}})_{A \rightarrow 2} - (\tilde{W}_A^{\text{ext}})_{B \rightarrow 2}^{\text{min}}$. Thus, equality holds in (B3) when B is on the minimal pathway $(A \rightarrow 2)^{\text{min}}$.

Because a non-equilibrium process changes as a function of time, it is more convenient to use the time derivative form of the above. Thus, for the process from A to B at times t and $t + dt$, where dt is infinitesimal time, we obtain the following inequality:

$$\frac{d\tilde{W}_A^{\text{ext}}(t)}{dt} \geq -\frac{d\Phi_A^{\text{neq}}(t)}{dt}. \quad (\text{B4})$$

This inequality extends the principle of minimum work to a non-equilibrium regime.

Although we have derived Eqs. (B3) and (B4) for the specific equilibrium state 2, the value $(\Phi_A^{\text{neq}})_A$ is the same for any quasi-equilibrium state along $\beta^{\text{qst}}(t)$ and $x^{\text{qst}}(t)$. To illustrate this, we introduce a third equilibrium state 3 and consider the transition $A \rightarrow 3$ (see Fig. 8). Because $(\tilde{W}_A^{\text{ext}})_{A \rightarrow 2}^{\text{min}} + (\tilde{W}_A^{\text{ext}})_{2 \rightarrow 3}^{\text{qst}} \geq (\tilde{W}_A^{\text{ext}})_{A \rightarrow 3}^{\text{min}}$ for $A \rightarrow 2 \rightarrow 3$ and $(\tilde{W}_A^{\text{ext}})_{A \rightarrow 3}^{\text{min}} + (\tilde{W}_A^{\text{ext}})_{3 \rightarrow 2}^{\text{qst}} \geq (\tilde{W}_A^{\text{ext}})_{A \rightarrow 2}^{\text{min}}$ for $A \rightarrow 3 \rightarrow 2$, we have

$$(W_A^{\text{ext}})_{A \rightarrow 2}^{\text{min}} + (\Phi_A^{\text{neq}})_2 = (W_A^{\text{ext}})_{A \rightarrow 3}^{\text{min}} + (\Phi_A^{\text{neq}})_3, \quad (\text{B5})$$

where we have used $(W_A^{\text{ext}})_{2 \rightarrow 3}^{\text{qst}} = (\Phi_A^{\text{qst}})_3 - (\Phi_A^{\text{qst}})_2$. From Eq. (B1), this indicates that the non-equilibrium Massieu potential is independent of the choice of the equilibrium state 2.

Because the other potentials are interrelated through TDL transformations, we obtain

$$\frac{d\tilde{W}_A^{\text{int}}(t)}{dt} \geq -\frac{d\Xi_A^{\text{neq}}(t)}{dt}, \quad (\text{B6})$$

$$\frac{d\tilde{Q}_A^{\text{ext}}(t)}{dt} \leq \frac{d\Lambda_A^{\text{neq}}(t)}{dt}, \quad (\text{B7})$$

and

$$\frac{d\tilde{Q}_A^{\text{int}}(t)}{dt} \leq \frac{d\Gamma_A^{\text{neq}}(t)}{dt}. \quad (\text{B8})$$

For an isothermal case, from the definitions $F_A^{\text{neq}}(t) = -\Phi_A^{\text{neq}}(t)/\beta$ and $G_A^{\text{neq}}(t) = -\Xi_A^{\text{neq}}(t)/\beta$, we have

$$\frac{dW_A^{\text{ext}}(t)}{dt} \geq \frac{dF_A^{\text{neq}}(t)}{dt} \quad (\text{B9})$$

and

$$\frac{dW_A^{\text{int}}(t)}{dt} \geq \frac{dG_A^{\text{neq}}(t)}{dt}. \quad (\text{B10})$$

However, unlike in the Massieu–Planck case, the equality in Eqs. (B9) and (B10) cannot be obtained in general because the minimum DL work path in Fig. 6 is evaluated by optimizing both $\beta(t)$ and $x(t)$, while β has been fixed to introduce the Helmholtz energy as $F_A^{\text{neq}}(t) = -\Phi_A^{\text{neq}}(t)/\beta$.

The above discussion indicates that the inclusion of the thermostatic process is a key to develop an efficient heat engine under non-equilibrium conditions.

Appendix C: Convexity of non-equilibrium thermodynamic potentials as functions of extensive variables

To obtain stable thermodynamic properties, the potential must be a convex function of the work variables. Even in the non-equilibrium case, we find that convexity holds under certain conditions. Here, we present this in the SB model. Because other potentials can be discussed

TABLE VII. Inequalities between the non-equilibrium state at time t_1 and the equilibrium state at time t_2 , with the conditions under which these inequalities hold. From these inequalities, we find that, for example, for a given inverse temperature and external field, the non-equilibrium Planck potential takes its maximum value when the state is in equilibrium.

| neq Potentials | Convexity and Concavity | Condition |
|----------------|--|---|
| Massieu | $(1 - \lambda)(\Phi_A^{\text{neq}})_A + \lambda(\Phi_A^{\text{neq}})_B \leq (\Phi_A^{\text{neq}})_\lambda$ | $\beta_A = \beta_B = \beta_\lambda$ |
| Planck | $(1 - \lambda)(\Xi_A^{\text{neq}})_A + \lambda(\Xi_A^{\text{neq}})_B \leq (\Xi_A^{\text{neq}})_\lambda$ | $\beta_A = \beta_B = \beta_\lambda$ and $\tilde{x}_A = \tilde{x}_B = \tilde{x}_\lambda$ |
| Helmholtz | $(1 - \lambda)(F_A^{\text{neq}})_A + \lambda(F_A^{\text{neq}})_B \geq (F_A^{\text{neq}})_\lambda$ | $\beta_A = \beta_B = \beta_\lambda$ |
| Gibbs | $(1 - \lambda)(G_A^{\text{neq}})_A + \lambda(G_A^{\text{neq}})_B \geq (G_A^{\text{neq}})_\lambda$ | $\beta_A = \beta_B = \beta_\lambda$ and $x_A = x_B = x_\lambda$ |

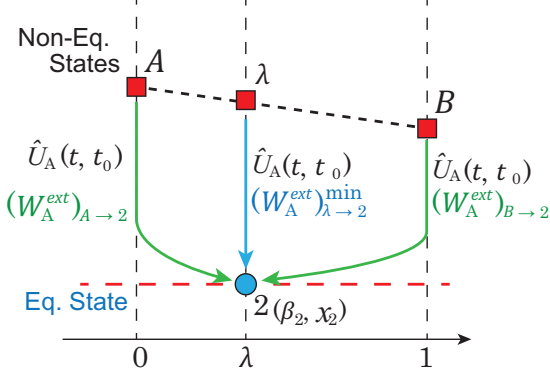


FIG. 9. Schematic for deriving convexity relations. The red squares represent the non-equilibrium states. The arrows are the relaxation paths to equilibrium state 2, as described by the time-evolution operator $\hat{U}_A(t, t_0)$: The blue arrow is the DL minimum work path from state λ .

similarly, we have limited our discussion to the case of non-equilibrium Massieu potential.

We consider three non-equilibrium states A , B , and λ ($\lambda \in [0, 1]$) with the same initial inverse temperature $\beta(t_0)$ at time t_0 . We then assume that the state λ satisfies the relation

$$(W_A)_\lambda = (1 - \lambda)(W_A)_A + \lambda(W_A)_B, \quad (\text{C1})$$

where $(W_A)_A = (W_A(p, q; t))_A$ and $(W_A)_B = (W_A(p, q; t))_B$ are the Wigner distributions in the quantum case (or phase space distributions in the classical case) in the A and B states. The time evolution operator of a subsystem is expressed as $\hat{U}_A(t, t_0) = \exp[-\int \hat{\mathcal{L}}(p, q) dt]$, where $\hat{\mathcal{L}}(p, q)$ denotes the Liouville operator, which includes fluctuation and dissipation operators for equilibration. In the quantum case, $\hat{\mathcal{L}}(p, q)$ acts on W_A , which is represented by hierarchical elements.^{39,40,66} We then obtain the relations between the extensive variable and internal energies as

$$(X_A)_\lambda(t) = (1 - \lambda)(X_A)_A(t) + \lambda(X_A)_B(t) \quad (\text{C2})$$

and

$$(U_A)_\lambda(t) = (1 - \lambda)(U_A)_A(t) + \lambda(U_A)_B(t), \quad (\text{C3})$$

where we have defined $(X_A)_\alpha(t) = \text{tr}_{\text{tot}}\{X_A(q)\hat{U}_{\text{tot}}(t, t_0)(W_{\text{tot}})_\alpha\}$ and $(U_A)_\alpha(t) = \text{tr}_{\text{tot}}\{[p^2/2m + U(q)]\hat{U}_{\text{tot}}(t, t_0)(W_{\text{tot}})_\alpha\}$ for $\alpha = A, B$, and λ . Thus, from Eq. (2), the DL extensive work $(W_A^{\text{ext}})_\alpha(t, t_0)$ ($\alpha = A, B$, and λ), performed between times t_0 and t also satisfies the equality

$$(W_A^{\text{ext}})_\lambda(t, t_0) = (1 - \lambda)(W_A^{\text{ext}})_A(t, t_0) + \lambda(W_A^{\text{ext}})_B(t, t_0). \quad (\text{C4})$$

The DL minimum work path from the state λ to the equilibrium state 2 is described by $\hat{U}_A(t, t_0)$ (see Fig. 9). This indicates that when t is large, the intensive variables must be $\beta(t) \rightarrow \beta_2$ and $x(t) \rightarrow x_2$, where β_2 and x_2 are the values at the equilibrium state 2. Therefore, processes starting from A and B also relax to the equilibrium state 2 as $t \rightarrow \infty$. Then, from Eq. (C4), we obtain

$$(W_A^{\text{ext}})_{\lambda \rightarrow 2}^{\text{min}} = (1 - \lambda)(W_A^{\text{ext}})_{A \rightarrow 2} + \lambda(W_A^{\text{ext}})_{B \rightarrow 2}. \quad (\text{C5})$$

Using the inequality $(W_A^{\text{ext}})_{\alpha \rightarrow 2} \geq (W_A^{\text{ext}})_{\alpha \rightarrow 2}^{\text{min}}$ for the states $\alpha = A$ and B and Eq. (B1), we obtain the inequality to prove convexity as

$$(1 - \lambda)(\Phi_A^{\text{neq}})_A + \lambda(\Phi_A^{\text{neq}})_B \leq (\Phi_A^{\text{neq}})_\lambda, \quad (\text{C6})$$

where $(\Phi_A^{\text{neq}})_\alpha$ is the non-equilibrium Massieu potential in the state α ($\alpha = A, B$, and λ). When A and B are in equilibrium, we obtain the convexity relation in the quasi-static case for a fixed inverse temperature using the inequality for the Massieu potential as Table VIII as⁶¹

$$(1 - \lambda)(\Phi_A^{\text{qst}})_A + \lambda(\Phi_A^{\text{qst}})_B \leq (\Phi_A^{\text{qst}})_\lambda. \quad (\text{C7})$$

The convexity and concavity properties for the other non-equilibrium thermodynamic potentials are summarized in Table VII.

Appendix D: Inequality between non-equilibrium and quasi-static thermodynamic potentials

Under given conditions, the non-equilibrium DL thermodynamic potentials are smaller than the quasi-static ones. Here, we derive the inequalities between the quasi-static and non-equilibrium thermodynamic potentials.

We consider a non-equilibrium-to-equilibrium transition $A \rightarrow 2$ from time t_1 to t_2 described by the inverse

TABLE VIII. Inequalities for Massieu–Planck potentials between the non-equilibrium state A at time t_1 and the equilibrium state 2 at time t_2 , together with the conditions under which these inequalities hold. From these inequalities, we find that, for example, for a given inverse temperature and intensive variable, the non-equilibrium Planck potential takes its maximum value when A is in the equilibrium state.

| neq Potentials | Inequalities | Condition |
|----------------|--|---|
| Massieu | $\Phi_A^{\text{qst}}(t_2) \geq \Phi_A^{\text{neq}}(t_1)$ | $\beta(t_1) = \beta(t_2)$ and $X_A(t_1) = X_A(t_2)$ |
| Planck | $\Xi_A^{\text{qst}}(t_2) \geq \Xi_A^{\text{neq}}(t_1)$ | $\beta(t_1) = \beta(t_2)$ and $\tilde{x}(t_1) = \tilde{x}(t_2)$ |
| C–Entropy | $\Lambda_A^{\text{qst}}(t_2) \geq \Lambda_A^{\text{neq}}(t_1)$ | $U_A(t_1) = U_A(t_2)$ and $X_A(t_1) = X_A(t_2)$ |
| B–Entropy | $\Gamma_A^{\text{qst}}(t_2) \geq \Gamma_A^{\text{neq}}(t_1)$ | $U_A(t_1) = U_A(t_2)$ and $\tilde{x}(t_1) = \tilde{x}(t_2)$ |

TABLE IX. Inequalities for Helmholtz–Gibbs potentials between the non-equilibrium state at time t_1 and the equilibrium state at time t_2 , with the conditions under which these inequalities hold.

| neq Potentials | Inequalities | Condition |
|-----------------|--|---|
| Helmholtz | $F_A^{\text{qst}}(t_2) \leq F_A^{\text{neq}}(t_1)$ | $T(t_1) = T(t_2)$ and $X_A(t_1) = X_A(t_2)$ |
| Gibbs | $G_A^{\text{qst}}(t_2) \leq G_A^{\text{neq}}(t_1)$ | $T(t_1) = T(t_2)$ and $x(t_1) = x(t_2)$ |
| Internal Energy | $U_A(t_2) \leq U_A(t_1)$ | $S_A^{\text{neq}}(t_1) = S_A^{\text{qst}}(t_2)$ and $X_A(t_1) = X_A(t_2)$ |
| Enthalpy | $H_A(t_2) \leq H_A(t_1)$ | $S_A^{\text{neq}}(t_1) = S_A^{\text{qst}}(t_2)$ and $x(t_1) = x(t_2)$ |

temperature $\beta(t)$ and the extensive variable $X_A^{\text{neq}}(t)$. The DL extensive work in this process is evaluated as

$$\int_{t_1}^{t_2} \left[U_A(t') \frac{d\beta(t')}{dt'} - \tilde{x}(t') \frac{dX_A^{\text{neq}}(t')}{dt'} \right] dt' = \tilde{x}_2 (X_A^{\text{neq}}(t_2) - X_A^{\text{neq}}(t_1)), \quad (\text{D1})$$

where we have assumed that $\beta(t) = \beta_2$ for time $t \geq t_1$ and $\tilde{x}(t) = \tilde{x}_2$ for time $t > t_1$ with the intensive variables β_2 and \tilde{x}_2 , allowing the subsystem to relax to the equilibrium state 2 at time t_2 . The value of \tilde{x}_2 is set to satisfy the condition $X_A^{\text{neq}}(t_2) = X_A^{\text{neq}}(t_1)$. Because $X_A^{\text{neq}}(t_2) = (X_A^{\text{qst}})_2 = X_A^{\text{neq}}(t_1)$, the right-hand side of Eq. (D1) vanishes. Thus, the net DL extensive work is zero, and so the DL minimum work principle reduces to $0 \geq (\Phi_A^{\text{neq}})_{A \rightarrow 2}$, from which it follows that $\Phi_A^{\text{qst}}(t_2) \geq \Phi_A^{\text{neq}}(t_1)$.

The inequalities for the other DL thermodynamic potentials were obtained in the same manner. The results are summarized in Tables VIII and IX

In Fig. 10, to illustrate the inequalities presented in Table VIII, we plot the difference between the quasi-static and non-equilibrium Planck potential, $\Delta \Xi_A(t) = \Xi_A^{\text{qst}}[\beta(t), \tilde{x}(t)] - \Xi_A^{\text{neq}}(t)$, for one cycle of the thermostatic Stirling engine described in Sec. III D. As can be seen, $\Delta \Xi_A(t)$ is always positive and satisfies the inequalities in Table VIII.

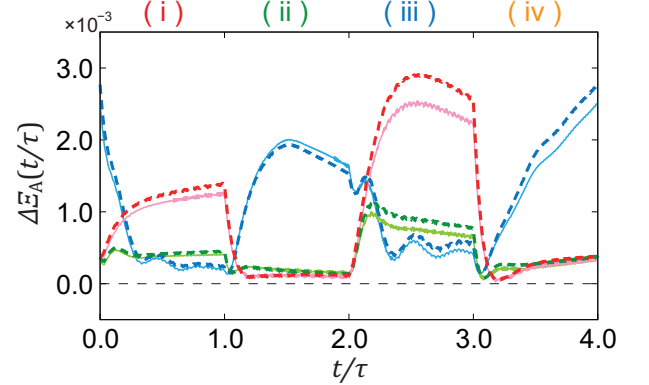


FIG. 10. Difference between the quasi-static and non-equilibrium Planck potentials in the quantum and classical cases (solid and dashed curves, respectively) for one cycle of the thermostatic Stirling engine. The blue, green, and red curves represent the weak ($A = 0.5$), intermediate ($A = 1.0$), and strong ($A = 1.5$) SB coupling, respectively.

¹S. Carnot, *Reflexions sur la puissance motrice du feu* (ChezBachelier Libraire, Quai des Augustins, Paris, 1824).

²H. T. Quan, Y. D. Wang, Y.-x. Liu, C. P. Sun, and F. Nori, “Maxwell’s demon assisted thermodynamic cycle in superconducting quantum circuits,” *Phys. Rev. Lett.* **97**, 180402 (2006).

³R. Kosloff and A. Levy, “Quantum heat engines and refrigerators: Continuous devices,” *Annual Review of Physical Chemistry* **65**, 365–393 (2014), pMID: 24689798.

⁴M. Esposito, M. A. Ochoa, and M. Galperin, “Nature of heat in strongly coupled open quantum systems,” *Phys. Rev. B* **92**, 235440 (2015).

⁵R. Schmidt, M. F. Carusela, J. P. Pekola, S. Suomela, and J. Ankerhold, “Work and heat for two-level systems in dissipative environments: Strong driving and non-Markovian dynamics,” *Phys. Rev. B* **91**, 224303 (2015).

⁶R. Uzdin, A. Levy, and R. Kosloff, “Equivalence of quantum heat machines, and quantum-thermodynamic signatures,” *Phys. Rev. X* **5**, 031044 (2015).

⁷R. S. Whitney, “Non-Markovian quantum thermodynamics: Laws and fluctuation theorems,” *Phys. Rev. B* **98**, 085415 (2018).

⁸H. T. Quan, Y.-x. Liu, C. P. Sun, and F. Nori, “Quantum thermodynamic cycles and quantum heat engines,” *Phys. Rev. E* **76**, 031105 (2007).

⁹K. Maruyama, F. Nori, and V. Vedral, “Colloquium: The physics of Maxwell’s demon and information,”

- Rev. Mod. Phys.* **81**, 1–23 (2009).
- ¹⁰K. Ono, S. N. Shevchenko, T. Mori, S. Moriyama, and F. Nori, “Analog of a quantum heat engine using a single-spin qubit,” *Phys. Rev. Lett.* **125**, 166802 (2020).
 - ¹¹L. M. Cangemi, V. Cataudella, G. Benenti, M. Sasseti, and G. De Filippis, “Violation of thermodynamics uncertainty relations in a periodically driven work-to-work converter from weak to strong dissipation,” *Phys. Rev. B* **102**, 165418 (2020).
 - ¹²P. Strasberg and A. Winter, “First and second law of quantum thermodynamics: A consistent derivation based on a microscopic definition of entropy,” *PRX Quantum* **2**, 030202 (2021).
 - ¹³M. Esposito, U. Harbola, and S. Mukamel, “Nonequilibrium fluctuations, fluctuation theorems, and counting statistics in quantum systems,” *Rev. Mod. Phys.* **81**, 1665–1702 (2009).
 - ¹⁴M. Campisi, P. Hänggi, and P. Talkner, “Colloquium: Quantum fluctuation relations: Foundations and applications,” *Rev. Mod. Phys.* **83**, 771–791 (2011).
 - ¹⁵T. Sagawa, “Second law-like inequalities with quantum relative entropy: An introduction,” (2023), [arXiv:1202.0983 \[cond-mat.stat-mech\]](https://arxiv.org/abs/1202.0983).
 - ¹⁶T. Schmiedl and U. Seifert, “Efficiency at maximum power: An analytically solvable model for stochastic heat engines,” *Europhysics Letters* **81**, 20003 (2007).
 - ¹⁷U. Seifert, “Stochastic thermodynamics, fluctuation theorems and molecular machines,” *Reports on Progress in Physics* **75**, 126001 (2012).
 - ¹⁸M. Esposito, K. Lindenberg, and C. V. den Broeck, “Entropy production as correlation between system and reservoir,” *New Journal of Physics* **12**, 013013 (2010).
 - ¹⁹M. Esposito and C. V. den Broeck, “Second law and landauer principle far from equilibrium,” *Europhysics Letters* **95**, 40004 (2011).
 - ²⁰A. Soret, V. Cavina, and M. Esposito, “Thermodynamic consistency of quantum master equations,” *Phys. Rev. A* **106**, 062209 (2022).
 - ²¹P. Strasberg, *Quantum Stochastic Thermodynamics: Foundations and Selected Applications* (Oxford University Press, 2022).
 - ²²R. Rao and M. Esposito, “Conservation laws shape dissipation,” *New Journal of Physics* **20**, 023007 (2018).
 - ²³C. Cockerell and I. J. Ford, “Stochastic thermodynamics in a non-markovian dynamical system,” *Phys. Rev. E* **105**, 064124 (2022).
 - ²⁴P. Talkner and P. Hänggi, “Colloquium: Statistical mechanics and thermodynamics at strong coupling: Quantum and classical,” *Rev. Mod. Phys.* **92**, 041002 (2020).
 - ²⁵R. Dann and R. Kosloff, “Unification of the first law of quantum thermodynamics,” *New Journal of Physics* **25**, 043019 (2023).
 - ²⁶A. Usui, K. Ptasiński, M. Esposito, and P. Strasberg, “Microscopic contributions to the entropy production at all times: from nonequilibrium steady states to global thermalization,” *New Journal of Physics* **26**, 023049 (2024).
 - ²⁷A. Ferreri, V. Macri, F. K. Wilhelm, F. Nori, and D. E. Bruschi, “Quantum field heat engine powered by phonon-photon interactions,” *Phys. Rev. Res.* **5**, 043274 (2023).
 - ²⁸S. Sakamoto and Y. Tanimura, “Numerically ”exact” simulations of entropy production in the fully quantum regime: Boltzmann entropy vs von Neumann entropy,” *The Journal of Chemical Physics* **153**, 234107 (2020), [arXiv:2012.09546](https://arxiv.org/abs/2012.09546).
 - ²⁹S. Sakamoto and Y. Tanimura, “Open quantum dynamics theory for non-equilibrium work: Hierarchical equations of motion approach,” *Journal of the Physical Society of Japan* **90**, 033001 (2021), [arXiv:2101.106307](https://arxiv.org/abs/2101.106307).
 - ³⁰A. Kato and Y. Tanimura, “Quantum heat transport of a two-qubit system: Interplay between system-bath coherence and qubit-qubit coherence,” *The Journal of Chemical Physics* **143**, 064107 (2015).
 - ³¹A. Kato and Y. Tanimura, “Quantum heat current under non-perturbative and non-Markovian conditions: Applications to heat machines,” *The Journal of Chemical Physics* **145**, 224105 (2016), [arXiv:1609.08783](https://arxiv.org/abs/1609.08783).
 - ³²A. J. Leggett, S. Chakravarty, A. T. Dorsey, M. P. A. Fisher, A. Garg, and W. Zwerger, “Dynamics of the dissipative two-state system,” *Rev. Mod. Phys.* **59**, 1–85 (1987).
 - ³³A. Caldeira and A. Leggett, “Path integral approach to quantum brownian motion,” *Physica A: Statistical Mechanics and its Applications* **121**, 587–616 (1983).
 - ³⁴H. Grabert, P. Schramm, and G.-L. Ingold, “Quantum brownian motion: The functional integral approach,” *Physics Reports* **168**, 115–207 (1988).
 - ³⁵U. Weiss, *Quantum Dissipative Systems*, 4th ed. (WORLD SCIENTIFIC, 2012).
 - ³⁶Y. Tanimura and R. Kubo, “Time evolution of a quantum system in contact with a nearly Gaussian-Markoffian noise bath,” *Journal of the Physical Society of Japan* **58**, 101–114 (1989).
 - ³⁷Y. Tanimura, “Nonperturbative expansion method for a quantum system coupled to a harmonic-oscillator bath,” *Phys. Rev. A* **41**, 6676–6687 (1990).
 - ³⁸Y. Tanimura, “Reduced hierarchical equations of motion in real and imaginary time: Correlated initial states and thermodynamic quantities,” *The Journal of Chemical Physics* **141**, 044114 (2014).
 - ³⁹Y. Tanimura, “Stochastic Liouville, Langevin, Fokker-Planck, and master equation approaches to quantum dissipative systems,” *Journal of the Physical Society of Japan* **75**, 082001 (2006).
 - ⁴⁰Y. Tanimura, “Numerically ”exact” approach to open quantum dynamics: The hierarchical equations of motion (HEOM),” *The Journal of Chemical Physics* **153**, 020901 (2020).
 - ⁴¹Y. Tanimura, “Real-time and imaginary-time quantum hierarchal Fokker-Planck equations,” *The Journal of Chemical Physics* **142**, 144110 (2015).
 - ⁴²T. Van Vu and K. Saito, “Thermodynamics of precision in markovian open quantum dynamics,” *Phys. Rev. Lett.* **128**, 140602 (2022).
 - ⁴³A. Ishizaki and Y. Tanimura, “Quantum dynamics of system strongly coupled to low-temperature colored noise bath: Reduced hierarchy equations approach,” *Journal of the Physical Society of Japan* **74**, 3131–3134 (2005).
 - ⁴⁴N. Makri, “Numerical path integral techniques for long time dynamics of quantum dissipative systems,” *Journal of Mathematical Physics* **36**, 2430–2457 (1995).
 - ⁴⁵N. Makri and D. E. Makarov, “Tensor propagator for iterative quantum time evolution of reduced density matrices. I. Theory,” *The Journal of Chemical Physics* **102**, 4600–4610 (1995).
 - ⁴⁶N. Makri and D. E. Makarov, “Tensor propagator for iterative quantum time evolution of reduced density matrices. II. Numerical methodology,” *The Journal of Chemical Physics* **102**, 4611–4618 (1995).
 - ⁴⁷M. Thorwart, P. Reimann, and P. Hänggi, “Iterative algorithm versus analytic solutions of the parametrically driven dissipative quantum harmonic oscillator,” *Phys. Rev. E* **62**, 5808–5817 (2000).
 - ⁴⁸V. Jadhao and N. Makri, “Iterative monte carlo for quantum dynamics,” *The Journal of Chemical Physics* **129**, 161102 (2008).
 - ⁴⁹N. Makri, “Blip decomposition of the path integral: Exponential acceleration of real-time calculations on quantum dissipative systems,” *The Journal of Chemical Physics* **141**, 134117 (2014).
 - ⁵⁰D. Segal, A. J. Millis, and D. R. Reichman, “Numerically exact path-integral simulation of nonequilibrium quantum transport and dissipation,” *Phys. Rev. B* **82**, 205323 (2010).
 - ⁵¹H.-D. Meyer, U. Manthe, and L. Cederbaum, “The multi-configurational time-dependent hartree approach,” *Chemical Physics Letters* **165**, 73–78 (1990).
 - ⁵²U. Manthe, H. Meyer, and L. S. Cederbaum, “Wavepacket dynamics within the multiconfiguration Hartree framework: General aspects and application to NOCl,” *The Journal of Chemical Physics* **97**, 3199–3213 (1992).

- ⁵³H. Wang and M. Thoss, “Quantum dynamical simulation of electron-transfer reactions in an anharmonic environment,” *The Journal of Physical Chemistry A* **111**, 10369–10375 (2007).
- ⁵⁴L. Song and Q. Shi, “Hierarchical equations of motion method applied to nonequilibrium heat transport in model molecular junctions: Transient heat current and high-order moments of the current operator,” *Phys. Rev. B* **95**, 064308 (2017).
- ⁵⁵H. Gong, Y. Wang, X. Zheng, R. Xu, and Y. Yan, “Nonequilibrium work distributions in quantum impurity system–bath mixing processes,” *The Journal of Chemical Physics* **157**, 054109 (2022).
- ⁵⁶C. L. Latune, G. Pleasance, and F. Petruccione, “Cyclic quantum engines enhanced by strong bath coupling,” *Phys. Rev. Appl.* **20**, 024038 (2023).
- ⁵⁷V. Boettcher, R. Hartmann, K. Beyer, and W. T. Strunz, “Dynamics of a strongly coupled quantum heat engine—Computing bath observables from the hierarchy of pure states,” *The Journal of Chemical Physics* **160**, 094108 (2024).
- ⁵⁸S. Koyanagi and Y. Tanimura, “The laws of thermodynamics for quantum dissipative systems: A quasi-equilibrium Helmholtz energy approach,” *The Journal of Chemical Physics* **157**, 014104 (2022), [arXiv:2205.09487](https://arxiv.org/abs/2205.09487).
- ⁵⁹S. Koyanagi and Y. Tanimura, “Numerically “exact” simulations of a quantum carnot cycle: Analysis using thermodynamic work diagrams,” *The Journal of Chemical Physics* **157**, 084110 (2022), [arXiv:2205.09487](https://arxiv.org/abs/2205.09487).
- ⁶⁰S. Koyanagi and Y. Tanimura, “Thermodynamic hierarchical equations of motion and their application to Carnot engine,” (2024).
- ⁶¹S. Koyanagi and Y. Tanimura, “Classical and quantum thermodynamics described as a system–bath model: The dimensionless minimum work principle,” *The Journal of Chemical Physics* **160**, 234112 (2024), [arXiv:2405.16787](https://arxiv.org/abs/2405.16787).
- ⁶²S. Koyanagi and Y. Tanimura, “Thermodynamic quantum Fokker–Planck equations and their application to thermostatic Stirling engine,” *The Journal of Chemical Physics* **161**, 112501 (2024), [arXiv:2408.01083](https://arxiv.org/abs/2408.01083).
- ⁶³P. Strasberg, G. Schaller, T. L. Schmidt, and M. Esposito, “Fermionic reaction coordinates and their application to an autonomous maxwell demon in the strong-coupling regime,” *Phys. Rev. B* **97**, 205405 (2018).
- ⁶⁴P. Strasberg and M. Esposito, “Measurability of nonequilibrium thermodynamics in terms of the hamiltonian of mean force,” *Phys. Rev. E* **101**, 050101 (2020).
- ⁶⁵J. Zhou, A. Li, and M. Galperin, “Quantum thermodynamics: Inside-outside perspective,” *Phys. Rev. B* **109**, 085408 (2024).
- ⁶⁶T. Ikeda and Y. Tanimura, “Low-temperature quantum Fokker-Planck and Smoluchowski equations and their extension to multistate systems,” *Journal of Chemical Theory and Computation* **15**, 2517–2534 (2019).
- ⁶⁷Y. Oono, *Perspectives on Statistical Thermodynamics* (Cambridge University Press, 2017).
- ⁶⁸H. R. Brown and J. Uffink, “The origins of time-asymmetry in thermodynamics: The minus first law,” *Studies in History and Philosophy of Science Part B: Studies in History and Philosophy of Biological and Biomedical Sciences* **35**, 1–24 (2004).
- ⁶⁹J. Uffink, “Bluff your way in the second law of thermodynamics,” *Studies in History and Philosophy of Science Part B: Studies in History and Philosophy of Biological and Biomedical Sciences* **35**, 25–49 (2004).
- ⁷⁰F. Massieu, “Sur les fonctions caractéristiques des divers fluides,” *CR Acad. Sci. Paris* **69**, 858–862 (1869).
- ⁷¹H. B. Callen, *Thermodynamics and an Introduction to Thermostatistics, 2nd Edition* (Wiley, 1991).
- ⁷²M. Planck, *Vorlesungen über Thermodynamik* (De Gruyter, 1922).
- ⁷³E. A. Guggenheim, *Thermodynamics: An Advanced Treatment for Chemists and Physicists* (North Holland, 1986).
- ⁷⁴R. Z, “Exergie, ein neues wort für „technische arbeitsfähigkeit,” *Forschung auf dem Gebiet des Ingenieurwesens A* **22**, 36–37.
- ⁷⁵P. Ullersma, “An exactly solvable model for brownian motion: I. derivation of the langevin equation,” *Physica* **32**, 27–55 (1966).
- ⁷⁶P. Ullersma, “An exactly solvable model for brownian motion: II. derivation of the fokker-planck equation and the master equation,” *Physica* **32**, 56–73 (1966).
- ⁷⁷Y. Tanimura and P. G. Wolynes, “Quantum and classical Fokker-Planck equations for a Gaussian-Markovian noise bath,” *Phys. Rev. A* **43**, 4131–4142 (1991).
- ⁷⁸Y. Tanimura and P. G. Wolynes, “The interplay of tunneling, resonance, and dissipation in quantum barrier crossing: A numerical study,” *The Journal of Chemical Physics* **96**, 8485–8496 (1992).
- ⁷⁹A. Kato and Y. Tanimura, “Quantum suppression of ratchet rectification in a Brownian system driven by a biharmonic force,” *The Journal of Physical Chemistry B* **117**, 13132–13144 (2013), [arXiv:1305.1402](https://arxiv.org/abs/1305.1402).